CFD Analysis of Ribbed Double Pipe Heat Exchanger

by

Mohamed Fathelrahman Mohamed

Dissertation submitted in partial fulfilment of

the requirements for the

Bachelor of Engineering (Hons)

(Mechanical Engineering)

JUNE 2009

Universiti Teknologi PETRONAS
Bandar Seri Iskandar
31750 Tronoh
Perak Darul Ridzuan

CERTIFICATION OF APPROVAL

CFD Analysis of Ribbed Double Pipe Heat Exchanger

by

Mohamed Fathelrahman Mohamed

A project dissertation submitted to the

Mechanical Engineering Programme

Universiti Teknologi PETRONAS

in partial fulfilment of the requirement for the

BACHELOR OF ENGINEERING (Hons)

(MECHANICAL ENGINEERING)

Approved by,

_____

(AP. Dr. Hussain H. Al-Kayiem)

UNIVERSITI TEKNOLOGI PETRONAS

TRONOH, PERAK

JUNE 2009

CERTIFICATION OF ORIGINALITY

This is to certify that I am responsible for the work submitted in this project, that the original work is my own except as specified in the references and acknowledgements, and that the original work contained herein have not been undertaken or done by unspecified sources or persons.

Mohamed Fathelrahman Mohamed

ABSTRACT

This study aims at simulating the flow in a ribbed double pipe heat exchanger both numerically and analytically and to analyze the accompanying thermo fluid mechanisms. Two procedures were developed to model the heat transfer and the pressure drop, analytical and numerical.

The analytical procedure employs empirical equations and correlations governing the flow. The equations were compiled in a MATLAB code to be solved. The numerical procedure is based on simulating the flow using FLUNET to obtain details of the velocity, temperature and pressure distribution across the flow channel. These values were then used to evaluate the friction factor and Stanton number from their fundamental relations using MATLAB

The results from both procedures showed good agreement with the experimental results. At a Reynolds number range of 2000-20,000 , heat transfer was found to be enhanced by more than 4 times at an expense of increasing pressure drop of more than 26 times.

ACKNOWLEDGMENT

I would like to express my heartfelt gratitude to the various people whose help and guidance allowed me to reach thus far with this project:

First and foremost, I would like to thank my supervisor AP. Dr. Hussain H. Al-Kayiem for his continuous guidance and relentless support. His passion for research has really inspired me. I am also deeply grateful for his advice, encouragement and patience throughout the duration of the project.

My sincere gratitude is extended to Dr. Ahmed Maher Said Ali, Mr. Rahmat Iskandar Khairul Shazi and Dr. Lau Kok Keong for the consultation they provided me throughout the project. Indeed, the assistance I received from each one of them contributed major milestones in the advancement of my research.

I also wish to thank Universiti Teknologi PETRONAS for providing the facilities to curry out this project.

To my beloved parents, my dear sister and brother, thank you for your endless love, support and encouragement.

TABLE OF CONTENTS

LIST OF TABLES

LIST OF FIGURES

NOMENCLATURE

LIST OF ABBREVIATIONS

A	Total heat transfer area.
A_f	Flow area.
C	Heat Capacity rate, mC_p.
C_P	Specific heat at constant pressure.
D	Diameter.
De	Equivalent diameter.
D_h	Hydraulic diameter.
d_i	Inner diameter of annular.
d_o	Outer diameter of annular.
e	Rib height.
e^+	Roughness Reynolds number.
f	Friction factor.
g	Acceleration of gravity.
h	Heat transfer Coefficient,
He^+	Heat transfer function.
k	Thermal Conductivity.
L	Flow section length.
$LMTD$	Log-mean temperature difference.
m	Mass flow rate.
P	Pressure.
A_P	Pressure drop.
Q	Heat transfer rate.
q	Flow rate.
Re^+	Roughness function.
r_i	Pipe inside radius.
r_o	Pipe outside radius.
T	Temperature.
T_f	Fluid temperature.
T_m	Average temperature.
U	Over all heat transfer Coefficient.
u	Local velocity in the X-direction.
u_c	Velocity at the centerline.

Greek Symbols

α	Flow angle of attack.
γ	Specific weight.
ε	Eddy diffusivity for heat transfer.
ε_m	Eddy diffusivity for momentum transfer.
η	Efficiency index.
μ	Dynamic viscosity:
υ	Kinematics viscosity.
π	3.14159
ρ	Density.

Subscripts And Superscripts

	Subscripts		Superscripts
a	Annular.	*	Dimensionless variable.
c	Cold.		
f	Fluid	+	law - of - the - wall variable
h	Hot.		
in	Inner, inlet.	-	Over bar, denotes mean or average value
o	Outer, Smooth.		
r	Ribbed.		
1	in.		
2	out.		

ii

CHAPTER 1

INTRODUCTION

1.1 BACKGROUND

A heat exchanger is an equipment in which heat is transferred from a hot fluid to a colder fluid. In most applications, the fluids do not mix but heat is transferred through a separating wall which takes on a wide variety of geometries. Heat exchangers are widely used in systems such as refineries, power plants, Oil Central Processing Facilities (CPF) and many other systems

The increasing cost of energy in the past few years arouse the need for using more efficient energy systems. This in turn encouraged researches in the field of augmenting or intensifying heat transfer in heat exchangers. Four techniques are recognized for the study of heat transfer enhancement, these are:

    i.   Continuously Supplied Augmentative Stimulation. (Fluid Additives)

    ii.   Turbulence Promotion.(Ribbing.... etc)

    iii.   Extended Heat Transfer Surfaces. (Finned Tubes)

    iv.   Enhanced Heat Transfer Surfaces (Material Properties)

1.2 PROBLEM STATEMENT

The increasing cost of energy in the past years aroused the need for using more efficient energy systems. This in turn encouraged researches in the field of augmenting heat transfer in heat exchangers. Several techniques are recognized for the study of heat transfer enhancement; out of which, ribbing is found to be a powerful heat transfer enhancing tool. Yet, most of the work performed in this area has thus far been mainly experimental with few numerical and analytical investigations.

1.3 OBJECTIVES

   i.   To analytically simulate a ribbed double pipe heat exchanger.

   ii.   To numerically simulate a ribbed double pipe heat exchanger.

   iii.   To analyze the thermo fluid mechanisms

   iv.   To investigate different ribbing configurations

1.4 SCOPE OF STUDY

In this project, the effect of various parameters on the friction factor as well as Stanton number is investigated. These parameters are: Reynolds number, rib height to Hydraulic Diameter ratio (e/D_h) and rib pitch to height ratio (P/e). The investigation is curried out using analytical and numerical techniques whose results are compared against previously obtained experimental data for validation.

1.4.1 Significance of the Study

Enhancing the performance of heat transfer media implies less heating energy to be needed. This will improve the overall efficiency of a given plant reducing its operating cost and ultimately, reducing the global costs of energy. Plants such as oil processing facilities, power plants, refineries...etc are all examples of plants that extensively use heat transfer principles in their operation which need to enhance the used heat transfer media

CHAPTER 2

LITERATURE REVIEW

An early study of the effect of roughness on friction and velocity distribution was experimentally performed by Nikuaradse [1] who is regarded as one of earliest contributors in the field.

Webb et al [2] in 1970 developed a number of correlations for heat transfer and fiction factor for turbulent flow in tubes having repeated-rib. He also developed a generalized understanding of the Stanton number and friction characteristics of repeated.

An important concept used to evaluate the overall effect of ribbing on the flow at different parameters was introduced by Webb [2]. This is the concept of annulus efficiency index which is the relative increase in friction necessary to achieve the desired heat transfer augmentation.

An interpretation for the heat transfer and pressure drop behavior in the presence of turbulators/ roughness elopements was presented by Takase in 1996, a [3,a] when he conducted an experimental and 2D/3D analysis on ribbed-roughened annulus flow. It attributes the heat transfer augmentation caused by the spacer rib to the increase of axial velocity due to a reduction in the channel cross section in the presence of ribs which promotes turbulence at earlier stages of the flow.

Later at the same year, Takase [3,b] developed a numerical technique for prediction of augmented turbulent heat transfer in an annular fuel channel with repeated two-dimensional square ribs in which a numerical model for predicting the Nussalt number was built. This work is a continuation of the previous work presented above of the same researcher. In this study an annular fuel channel with square repeated 2D ribs model was experimentally analyzed. Results of the experimental analysis were compared against a numerical model consisting of five equations proposed to predict the Nu for the flow. These equations were solved using FLUENT. The proposed equations revealed matching results to the experimental ones.

3

In 1998 [4], Yildiz et al studied the effect of twisted strips on the heat transfer and pressure drop in heat exchangers. They have conducted an experimental study on double pipe heat exchangers with both parallel and counter flow cases. Experiments for the previous cases were conducted on smooth and roughened pipe. Roughening effect was achieved by placing twisted narrow, thin metallic strips at the inner pipe surface. Reynolds's number in these experiments was in the range of 3400-6900 and the results have shown an increase in the heat transfer up to 100% at a cost of 130% increase in the pressure drop. They have concluded that: The heat transfer rates in double-pipe air cooling systems may be increased by up to 100% by placing twisted strip turbulators inside the tubes. Moreover, further improvements in heat transfer may be acquired with increasing pitch size. Turbulators cause a considerable increase in pressure drop, but the heat equivalent of this energy loss is negligible in comparison with the heat gained by the turbulators.

In 1999 [5], Braun et al performed experimental and numerical investigation on turbulent heat transfer in a channel with periodically arranged rib roughness elements. The experiments were carried out on a Reynolds's number of 6000. The numerical analysis was carried out using Large Eddy Simulation (LES). The results obtained from this study has shown that even at the eighth periodic roughness element, turbulent flow conditions were not developed which is mainly attributed to the fact that the height of the element used in the study was not large enough to produce the anticipated effect.

Another study was carried out in the year 1999 [6] by Al-Habeeb, on the effect of ribbing on the parallel flow of double pipe heat exchangers. The study which was conducted experimentally investigated two main cases, when hot flow is at the annulus and when the cold flow is at the annulus. Reynolds's number used was in the range of (10000-72000) for the pipe flow and of (2600-20000) for the annular flow for the first case and for the second case ranges of (12000-70000) and (4500-17000) were used for the pipe and the annulus respectively. The results obtained from this study show that when the hot flow is inside the pipe, heat transfer enhancement of 4.26 was achieved while when the hot flow is in the annulus, enhancement of up to 4.4 was achieved.

In 2007 [7], Hacı et al studied the effect of variable fin inclination angle on the thermal behavior of a plate fin-tube heat exchanger. The study was performed

numerically using a 3-D model using GAMBIT software to create the model and produce the meshing while FLUENT software was used to perform the numerical analysis. The analysis was performed on a steady state, laminar flow with fin angles varying from 0° to 30° with an increment of 5°. Results from this work shows that heat transfer enhancement and effectiveness improvement were optimum at inclination angle of 30° where heat transfer improvement was recorded to be 105.24% while accompanying pressure drop was found negligible.

In 2008 [8], Al-Kayiem and Al-Habeeb conducted a numerical study on the effect of various ribbing configurations on the heat transfer. The study aimed to compare the experimental results obtained in number [6] with the numerical results. The study revealed good agreement between the experimental work and the numerical correlations used

In 2008 [9], Ozxeyhan et al investigated numerically the heat transfer enhancement in a tube using circular rings separated from the wall. This study differs from other studies in the field in that the ribs here were not attached to the wall so that heat transfer enhancement is solely due to disturbing of the laminar sub layer. The study was carried out using FLUENT code and it was on a range of Reynolds number of (4400-43000). Results from this study shown that heat transfer enhancement increases with the pitch of the ribs.

CHAPTER 3

METHODOLOGY

3.1 ANALYSIS TECHNIQUE

The figures below illustrate the geometry of the investigated heat exchanger with the nomenclature for the rib height (e) and the pitch distance (P).

e/D RELATIVE ROUGHNESS
p/e RELATIVE RIB SPACING
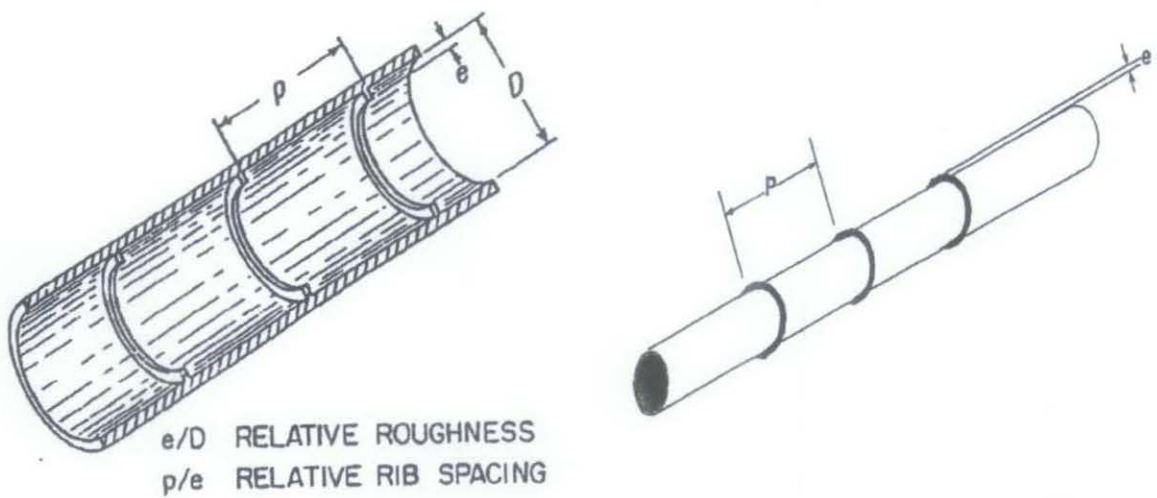
Figure 1   The geometry of the heat exchanger and the related nomenclature

Two techniques were adopted to model the flow inside the heat exchanger. First, the empirical equations and correlations explained in chapter 4 were gathered from the literature and a MATLAB code was the developed to solve them. The second technique is the numerical analysis. The heat exchanger was first modeled on ATUTO CAD to create the geometry in 3D. This geometry was then imported into GMABITI for mesh generation and boundary conditions definition. Following to that, it was exported to FLUENT to run the simulation. Simulations were run for the smooth case at the beginning followed by the various ribbing cases. Stanton number and friction factor were evaluated using the procedure explained in chapter 5. Inputs to these equations are the pressure drop and temperatures evaluated numerically through the simulations. The various ribbing configurations investigated are summarized by the following table and figure. *(Appendix A details the studied cases and their respective parameters)*

Case	e/Dh	P/e	Analysis Procedure	
			Numerically	Analytically
case 1	0.0595	10	X	X
case 2	0.0595	15	X	X
case 3	0.1070	10	X	X
case 4	0.0595	20		X
case 5	0.0765	10		X
case 6	0.0765	15		X
case 7	0.0765	20		X
case 8	0.1070	15		X
case 9	0.1070	20		X

Table 1   Summary of the ribbing configurations investigated

Figure 2   Sample of the ribbing configuration considered

3.2 TOOLS AND SOFTWARES

All simulations and MATLAB analysis were run on a computer with the following specifications:

- Processor   : Dual Core, 2.0 GHz
- RAM   : 2 GB

A number of softwres were used in the current analysis as explained in the previous sections. A list of all softwares is given below:

   i.   AUTOCAD

   ii.   GAMBIT

   iii. FLUNET

   iv. MATLAB

3.3 FLOW CHARTS

The flowcharts in the following pages illustrate the methodology adopted for both the analytical and numerical procedures.

START

Evaluate St for smooth case (eqn 4)

Evaluate f for smooth case (eqns 1,2)

Put e+ = 1

Calclate f_r (eqns 5,6)

Calculate e_c^+ (eqn 7)

NO

if $(|e_c^+ - e^+|) / e^+$ ≤0.001

YES

Calculate St_r (eqns 9,10)

END
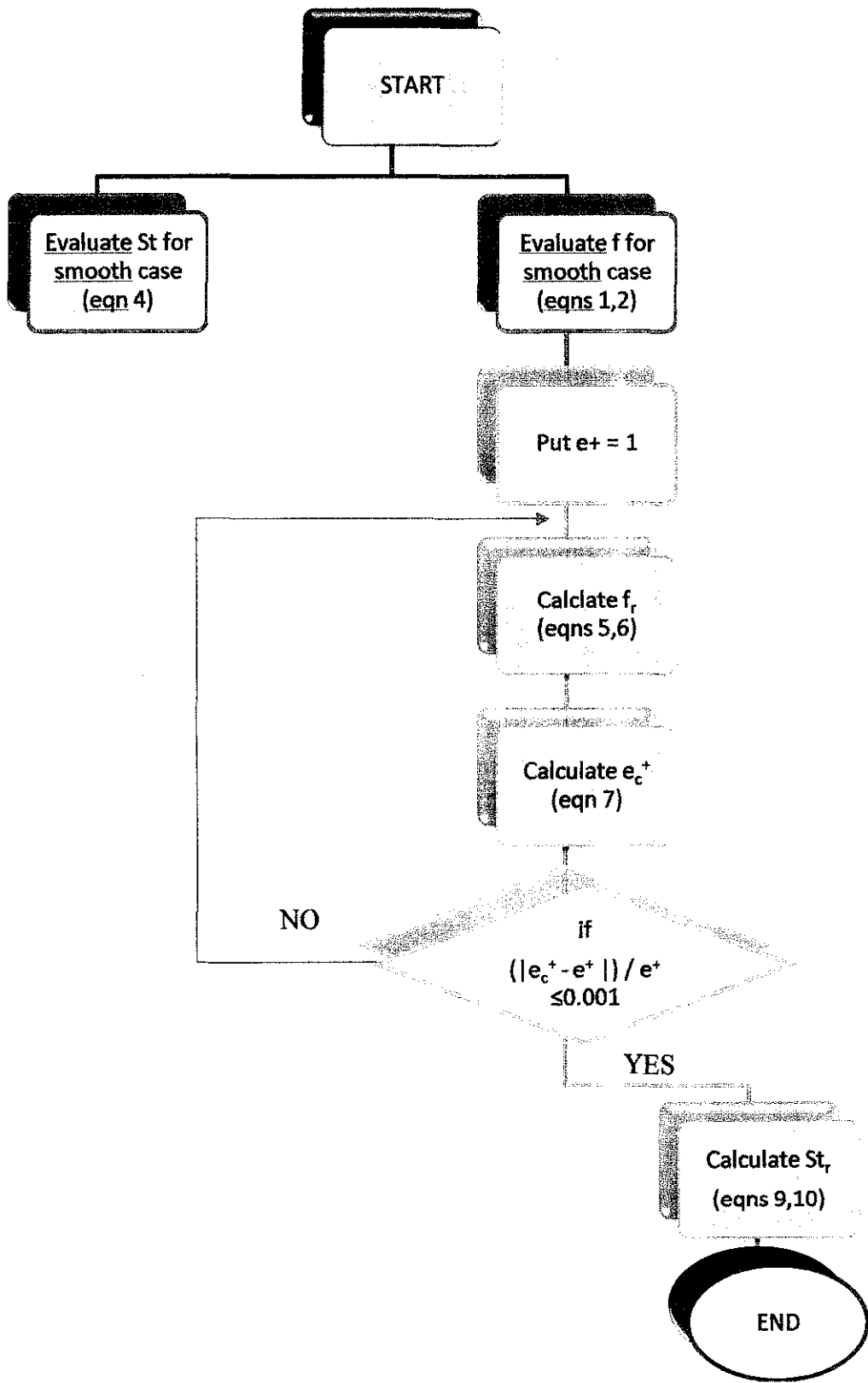
Figure 3   Methodology of the analytical procedure
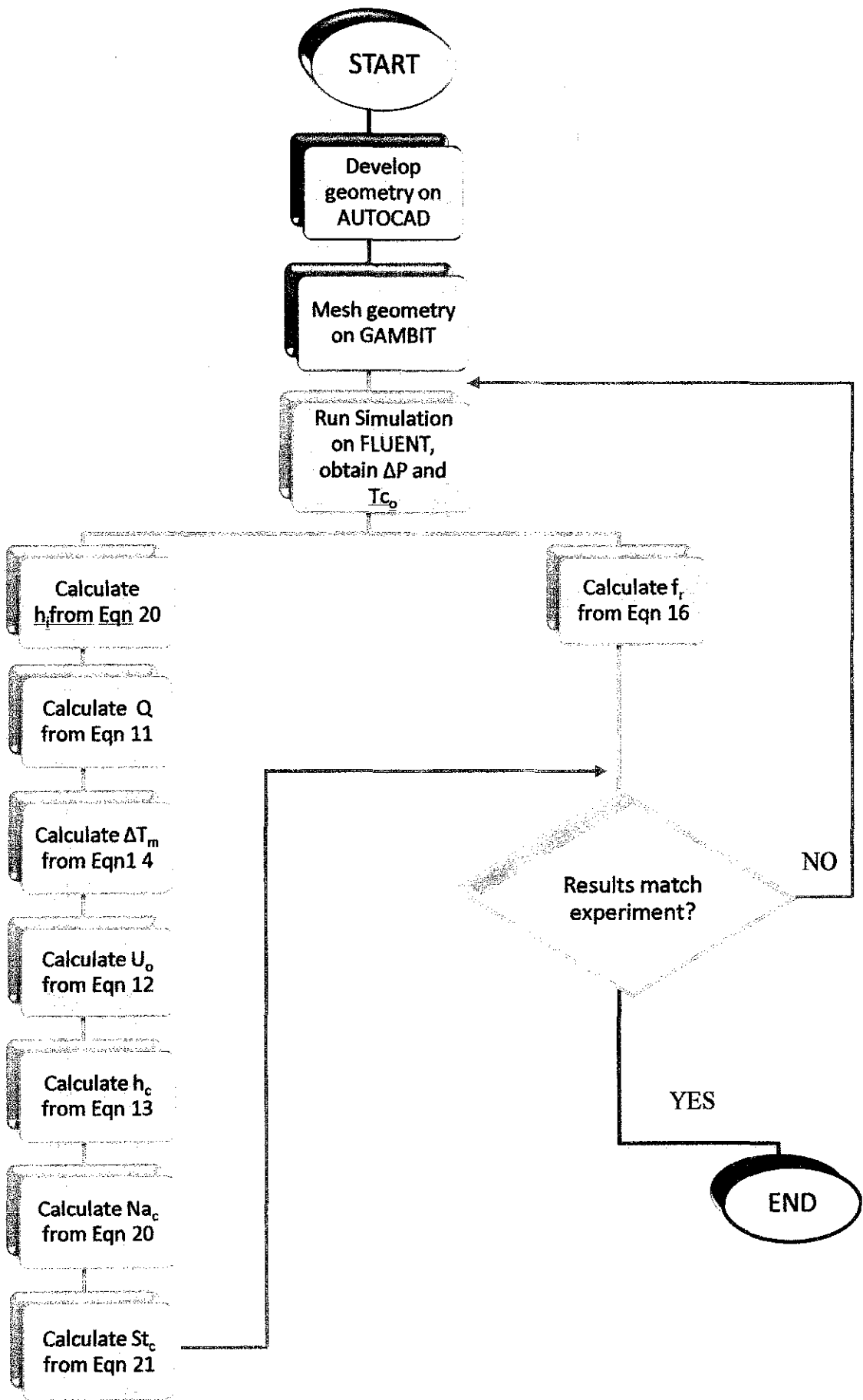
Figure 4   Methodology of the CFD procedure

3.3.1 Work Plan Gantt chart

No.	Detail/ Week	1	2	3	4	5	6	7	8	9	10	11	12	13	14
1	Smooth Case Simulation	■	■	■											
2	Submission of Progress Report 1				●										
3	Ribbed Case Simulation				■	■	■	■							
4	Submission of Progress Report 2								●						
5	Seminar (compulsory)								●						
5	Rib Shape angle and attack angle study								■	■	■	■			
6	Poster Exhibition										●				
7	Submission of Dissertation (soft bound)												●		
8	Oral Presentation													●	
9	Submission of Project Dissertation (Hard														●

●   Suggested Milestone

■   Process

CHAPTER 4

ANALYTICAL ANALYSIS

4.1 FRICTION FACTOR FOR SMOOTH CASES, f

Two correlations were used to evaluate the friction factor wherein the values are selected with correspondence to the Re value. These correlations are as follows:

- Blasius correlation (Kakac [10]):

$$f = 0.0791 \cdot \text{Re}^{-0.25} \quad 4 \times 10^3 \le \text{Re} \le 10^5 \quad (1)$$

- Drew, Koo and McAdams correlation (Kakac [10]):

$$f = 0.0014 + 0.125.\text{Re}^{-0.32} \quad 4 \times 10^4 \le \text{Re} \le 10^6 \quad (2)$$

The previous correlations evaluate the friction factor as a function of Reynolds number only.

4.2 THE CONVECTIVE HEAT TRANSFER FOR NON-RIBBED ANNULUS CASES, St:

The same equations mentioned in section 3.1.3 are used, they repeated below:

$$Nu = \frac{h_i D}{k} = 0.023 \text{Re}^{0.8} \text{Pr}^n \qquad (3)$$

and the exponent, n has values of:

$$n = \begin{cases} 0.4 & \textit{for heating} \\ 0.3 & \textit{for cooling} \end{cases}$$

$$St = \frac{Nu}{\text{Re Pr}} \qquad (4)$$

4.3 FRICTION FACTOR FOR RIBBED ANNULUS CASES, fr:

By combining the velocity defect law for pipe flow with the law of the wall, Nikuradse [1], developed the "friction similarity law" for sand grain roughness. This can be assumed to hold for the entire cross section of the flow. To satisfy the ribbed annulus flow, the average surface roughness, ε is replaced by the rib height, e. The Roughness function, Re^+ is obtained as:

$$Re^+\left(e^+\right)=\left(\frac{2}{f_r}\right)^{0.5}+2.5\ln\left(\frac{2e}{D_h}\right)+3.75 \qquad (5)$$

where, the roughness Reynolds number, e^+ is:

$$e^+=\frac{e}{D_h}\cdot Re\cdot\left(\frac{f_r}{2}\right)^{0.5} \qquad (6)$$

Han [11] recommended a correlation for the friction factor for turbulent flow between parallel plates with repeated-rib roughness by taking into account the geometrically non similar roughness parameters of P/e, rib shape, Φ and the angle of attack, α, as:

$$Re^+\left(e^+\right)=\frac{\left[4.9\left(\frac{e^+}{35}\right)^m\right]}{\left[\left(\frac{\phi}{90^o}\right)^{0.35}\left(\frac{10}{(P/e)}\right)^n\left(\frac{\alpha}{45^o}\right)^{0.57}\right]} \qquad (7)$$

where the exponents m, n are given as follows:

$$m = -0.4 \qquad \text{if} \qquad e^+ < 35$$

$$m = 0 \qquad \text{if} \qquad e^+ \geq 35$$

$$n = -0.13 \qquad \text{if} \qquad P/e < 10$$

$$n=0.53\left(\frac{\alpha}{90^o}\right)^{0.71} \qquad \text{if} \qquad P/e \geq 10$$

Equations, 16, 17, and 18 were solved iteratively by using initial guess of $e^+ = 1$ and substituting into equation 17. Re^+ is substituted for from equation 18. Iterations were performed until residues fell below 0.001.

4.4 HEAT TRANSFER FOR RIBBED ANNULUS CASE, St_r:

Han et al. [11] and Webb et al. [12] proposed a formula that applies the heat and momentum transfer analogy known as " Heat Transfer Similarity Law" as follows:

$$\frac{\left(\dfrac{f_r}{2St}\right)-1}{\left(\dfrac{f_r}{2}\right)^{0.5}}+\mathrm{Re}^+ = He^+\left(e^+,\mathrm{Pr}\right) \qquad (8)$$

where, He^+, Re^+ and f_r are known, - f_r is calculated as in subsection 3.2.3 above- , then Stanton number in the ribbed flow could be evaluated as:

$$St_r = \frac{f_r}{\left(He^+ - \mathrm{Re}^+\right)\cdot\left(2f_r\right)^{0.5}+2} \qquad (9)$$

Values of He^+ can be found using the following correlation recommended by Webb et al. [12]

$$He^+ = 4.5\cdot\left(e^+\right)^{0.28}\left(\mathrm{Pr}\right)^{0.57} \qquad (10)$$
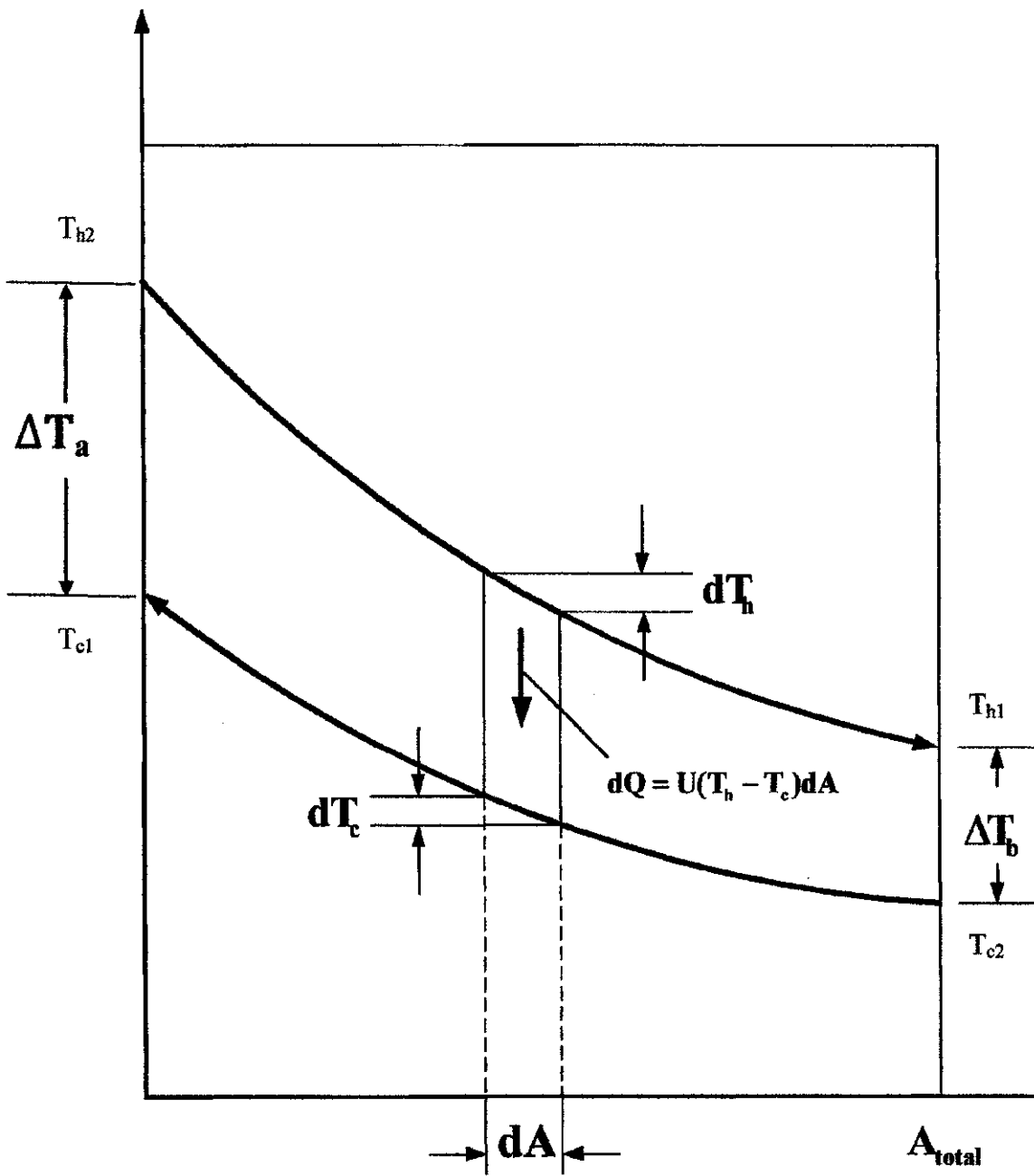
Figure 5   Temperature distribution across the heat exchanger

CHAPTER 5

NUMERICAL ANALYSIS

5.1 OVERALL HEAT TRANSFER

The total heat transferred from the hot fluid in the pipe to the cold fluid in the annulus is given by the relation:

$$Qh = mh\,Cph\,(Th1 - Th2) = Qc = mc\,Cpc\,(Tc2 - Tc1) \qquad (11)$$

The total heat transferred is also given using the overall heat transfer coefficient as follows:

$$Q = Uo\,A\,\Delta Tm \qquad (12)$$

Where:

A is the total heat transfer area – the outer surface of the pipe in this case –

U_o is the overall heat transfer coefficient based on the outer surface area of the pipe;

$$Uo = \frac{1}{\left[\left(\frac{ro}{ri\,hi}\right) + \left(\frac{ro}{km}\right)Ln\frac{ro}{ri} + \frac{1}{ho}\right]} \qquad (13)$$

ΔT_m is the log mean temperature difference across the pipe; if subscripts a, b indicate the pipe inlet and outlets respectively, then ΔT_m is given by:

$$\Delta Tm = \frac{\Delta Tb - \Delta Ta}{Ln\frac{\Delta Tb}{\Delta Ta}} \qquad (14)$$

5.2 FRICTION FACTOR, f:

In fully developed flow in closed conduits, either laminar or turbulent, the pressure drop varies with inertia force parameters, shear force parameters and the surface conditions as:

$$\frac{\Delta p}{L} = \Phi(u_m, \rho, D, \mu, \varepsilon) \qquad (15)$$

Where, ε is the absolute roughness of the conduit surface having dimensions of length. μ and ρ are the fluid viscosity and density, respectively and u_m is the mean velocity. Using dimensional analysis and adopting the hydraulic diameter criteria, D_h instead of the pipe diameter, D, getting the known Darcy Weisbach equation from which the friction factor, f in the annular flow is:

$$f = \frac{\Delta p}{\left(\dfrac{4L}{D_h}\right)\left(\dfrac{\rho u_m^2}{2}\right)} \qquad (16)$$

Where, the hydraulic diameter for the annulus is:

$$D_h = \frac{4\left(\dfrac{\pi}{4}\right)(d_o^2 - d_i^2)}{\pi d_o + \pi d_i} = d_o - d_i \qquad (17)$$

The outlet pressure is evaluated either from the experiment or from the simulation results. Inlet pressure on the other hand is evaluated knowing that pumping power used for the experiment was 5 hp, with efficiency of 65%. The pressure is then calculated using the formula:

$$\eta = \frac{q\,Pi}{p} \qquad (18)$$

Where η is the pumping efficiency;

Q is the fluid flow rate;

P_i is the inlet pressure;

P is the pumping power in KW.

5.3   THE CONVECTIVE HEAT TRANSFER, St:

The coefficient of convective heat transfer, h is a function of many variables such as the geometry of the flow passage, the surface roughness, the flow direction and velocity, temperatures of the fluid and the surface and the fluid properties (density, viscosity, heat capacity and the thermal conductivity). The differential equations of convection are of the most difficult class and the empirical treatment is not entirely satisfactory, but yields adequate results. Accordingly, treatment of the above set of

17

variables by dimensional analysis method has led to number of correlations in the form of:

$$Nu = Nu(\text{Re}, \text{Pr}) \qquad (19)$$

For fully developed turbulent flow in pipes with $\varepsilon / D < 0.001$, the following correlation is recommended by Dittus and Boelter as mentioned by [10]:

$$Nu = \frac{h_i D}{k} = 0.023 \text{Re}^{0.8} \text{Pr}^n \qquad (20)$$

and the exponent, n has values of:

$$n = \begin{cases} 0.4 & \text{for heating} \\ 0.3 & \text{for cooling} \end{cases}$$

The equation is used in the present annulus flow by using D_h instead of D. The physical properties were evaluated at the mean bulk temperature. Accordingly,

$$St = \frac{Nu}{\text{Re} \, \text{Pr}} \qquad (21)$$

5.4 GEOMETRY CREATION

All geometries were created in 3D domain using AUTOCAD for ease of handling. The geometries were then exported to GAMBIT. The actual geometry consists of 4 different volumes however the volume which represents the cold water in the annulus was created alone where the focus is laid upon the flow in the annulus alone. Thus, volumes representing wall thicknesses as well as the hot water inside the inner pipe were not created. This measure is taken to simplify the geometry and to reduce computational time. Proper assumptions as well as boundary conditions were applied to counter for the simplified geometry as will be explained in the following sections. The following figures illustrate the geometry as created in AUTOCAD.
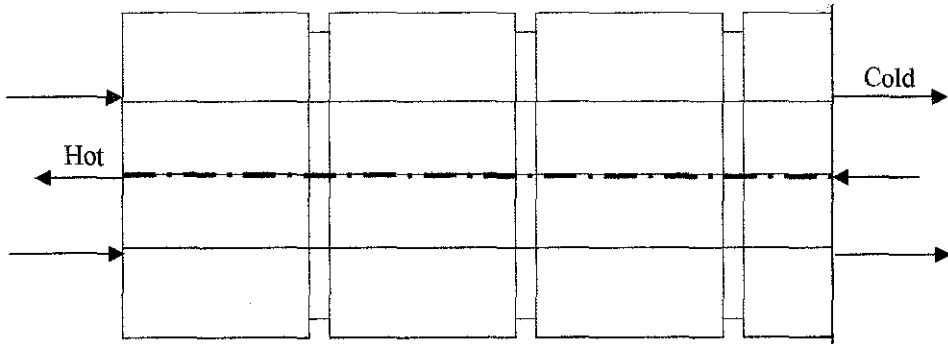
Figure 6   2D Sample of the geometry

18
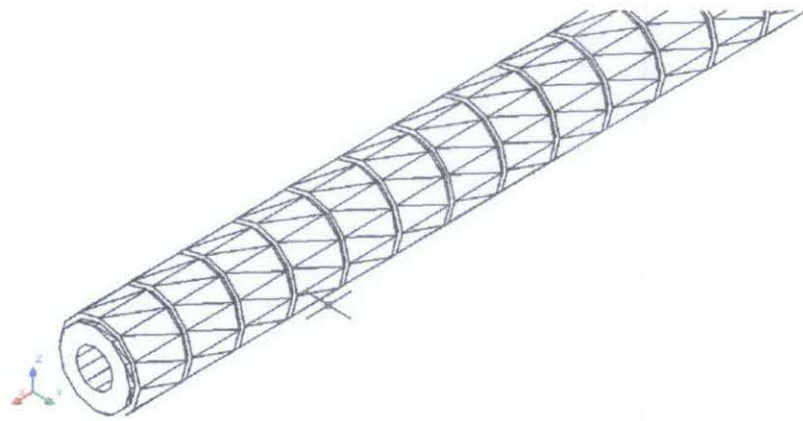
Figure 7   A 3D sample of the geometry

5.5   MESH GENERATION

The geometry was meshed using the volume meshing tool. Only one element type was sucessfully applied that is the Tetrahedral type. Errors were received when attmpteing to use any other element type. This is believed to be a result of the complex interior of the geometry due to the presence of the ribs. Interval size used is 0.55 units and the total number of elements created is 293,104 elments.
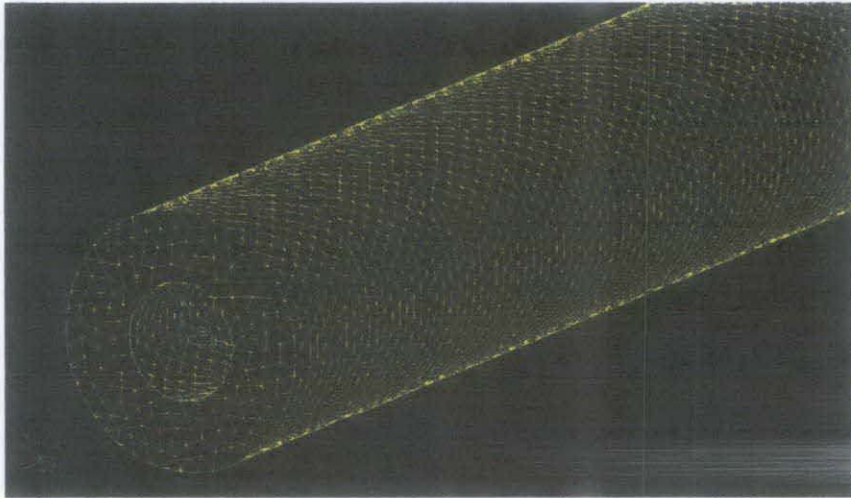
Figure 8   Sample of the meshed geometry

5.5.1   Boundary Conditions

In all of the investigated cases, the pressure at outlets is unknown and therefore it is not possible to use a boundary condition which uses pressure as a user input. Hence, Velocity inlet is used for the flow inlets in the annulus and outflow is used for the outlets. The outer walls were set as walls with no thermal conditions.

19

The inner wall separating annulus from inner pipe contains a thermal boundary condition. This boundary condition is either to be set by the user or to be left to the simulation to evaluate. In the latter case, other inputs are required such as outlet pressure which is unknown. Due to the several unknowns in the problem, an assumption was made that the heat flows uniformly from the hot pipe to the cold annulus throughout the heat transfer area. With that assumption, the heat flux is calculated from the experimental data using the formula below:

$$\phi = \frac{m\ cp\ \Delta T}{A}$$

The calculated value is used as a thermal condition input to the simulation. Now, since the heat flux value is predetermined, there is no needed for the solver to perform any calculations on the inner pipe and since it is the annulus in which the study is interested, the inner pipe geometry was not created. This would save the calculation resources and reduce the simulation time,

5.6 SIMULATION SET UP

All simulations were run on FLUENT 6.2 using the 3D Double Precision mode (3DPP). The following sub section illustrates the turbulence model employed and the relevant equations.

5.6.1 The Turbulence Model

Reynolds averaging of the Navier-Stocks equations was employed to solve the turbulent model wherein, the instantaneous (exact) Navier-Stokes equations are decomposed into the mean (ensemble-averaged or time-averaged) and fluctuating components in the general form for a given quantity ϕ:

$$\phi = \overline{\phi} + \phi' \qquad (22)$$

The Navier-Stocks equations in the averaged form can be written as:

$$\frac{\partial \rho}{\partial t} + \frac{\partial}{\partial x_i}(\rho u_i) = 0 \qquad (23)$$

$$\frac{\partial}{\partial t}(\rho u_i) + \frac{\partial}{\partial x_j}(\rho u_i u_j) = -\frac{\partial p}{\partial x_i} + \frac{\partial}{\partial x_j}\left[\mu\left(\frac{\partial u_i}{\partial x_j} + \frac{\partial u_j}{\partial x_i} - \frac{2}{3}\delta_{ij}\frac{\partial u_l}{\partial x_l}\right)\right] + \frac{\partial}{\partial x_j}(-) \qquad (24)$$

20

The model used is the RNG k-ε model which is derived using the statistical technique (called renormalization group theory) and contains an extra term in its ε equation which improves its accuracy. The transport equations (K-ε) are as follows:

$$\frac{\partial}{\partial t}(\rho k) + \frac{\partial}{\partial x_i}(\rho k u_i) = \frac{\partial}{\partial x_j}\left(\alpha_k \mu_{eff}\frac{\partial k}{\partial x_j}\right) + G_k + G_b - \rho \epsilon - Y_M + S_k \quad (25)$$

and

$$\frac{\partial}{\partial t}(\rho \epsilon) + \frac{\partial}{\partial x_i}(\rho \epsilon u_i) = \frac{\partial}{\partial x_j}\left(\alpha_\epsilon \mu_{eff}\frac{\partial \epsilon}{\partial x_j}\right) + C_{1\epsilon}\frac{\epsilon}{k}(G_k + C_{3\epsilon}G_b) - C_{2\epsilon}\rho\frac{\epsilon^2}{k} - R_\epsilon + S_\epsilon \quad (26)$$

The main difference between the RNG and standard k-ε models lies in the additional term in the ε equation given by

$$R_\epsilon = \frac{C_\mu \rho \eta^3 (1 - \eta/\eta_0)}{1 + \beta \eta^3}\frac{\epsilon^2}{k} \quad (27)$$

Where

$$\eta \equiv Sk/\epsilon, \ \eta_0 = 4.38, \ \beta = 0.012.$$

The equations' constants were left at their default values set by FLUENT 6.2 as follows: $C_{1\epsilon}$ = 1:42; $C_{2\epsilon}$ = 1:68. For the turbulence intensity, Versteeg and Malalasekera [13] recommended using values of no greater than 10% for high turbulent flow while using values between 1-5% for less turbulent flow. Based on this the turbulence intensity was set to 3% for the smooth case and 10% for the ribbed cases.

Versteeg and Malalasekera [13] also recommended the use of QUICK descretisation scheme (Quadratic Upstream Interpolation for Convective Kinetics) yet, the QUICK scheme is not available under FLUENT 6.2 and therefore the second order upwind discretisation was applied to all equations instead.

Default convergence criteria were used where it is set at 0.001 for all equations except for the energy equation which is set to 10^{-6}. Convergence was reported after 100 to 200 iterations. A sample of the residuals is shown below.

21
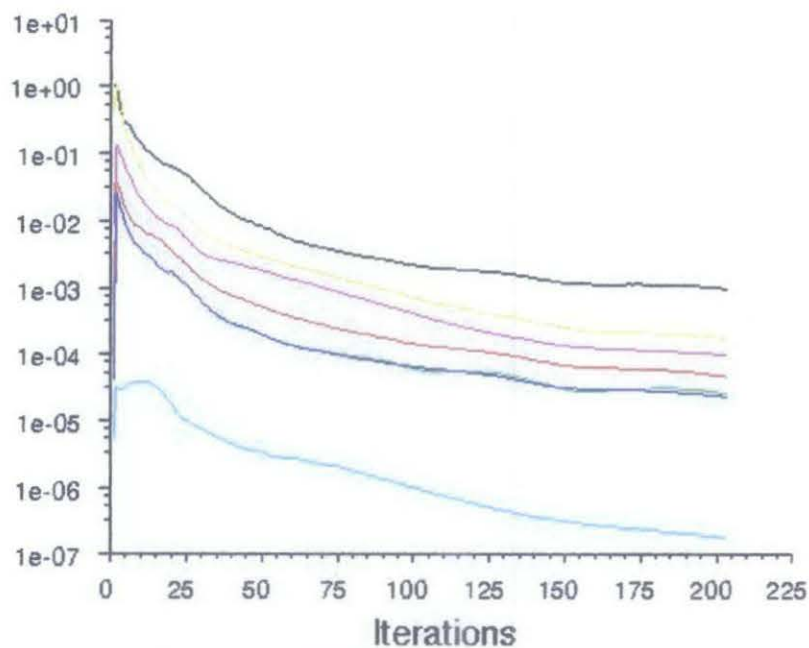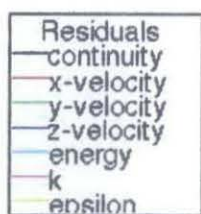
Figure 9   Sample of Residuals
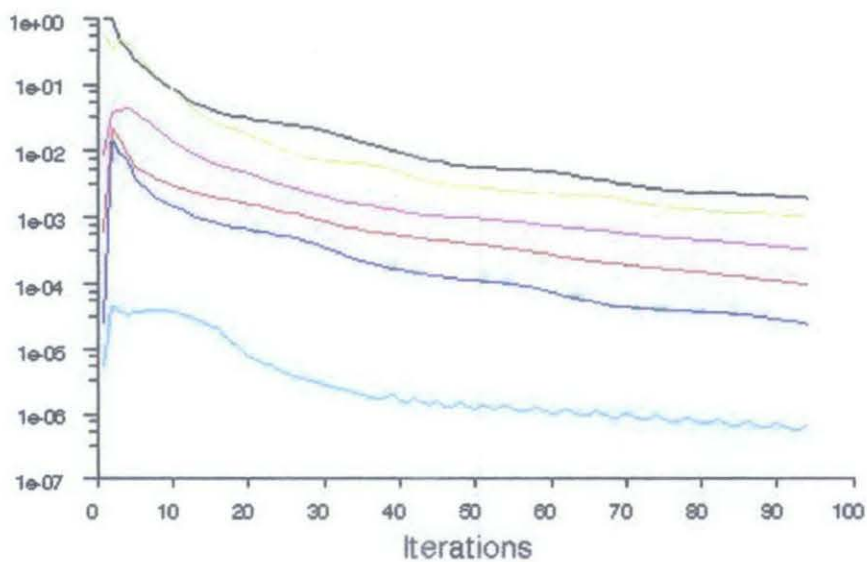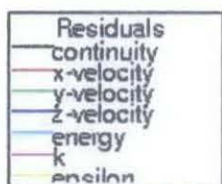
Figure 10   Sample of residuals

22

5.6.2 Grid Independency Check

To confirm that the obtained numerical results are valid in view of the used conditions, grid independency check is run. That is running the simulation at different meshing arrangements (e.g. element type, mesh size... etc) and check if the same results are obtained. As mentioned in the mesh creation section, only one mesh element type was able to be used without an error, that is the tetrahedral element and therefore, nothing can be done on the element type. The mesh size was then increased gradually up to 0.2 under which the number of elements reached 916,000. The simulation was run again using this mesh. Results with negligible difference were obtained. The mesh size was then decreased down to 0.5. results in this case showed significant change and hence it is concluded that the minimum size suitable is o.55. The following table shows a sample comparison for outlet temperature and ΔP for smooth case 6 between coarse, original and refined meshes. The consistency of the results at higher mesh sizes indicates that the obtained solution is independent of the mesh and it is correct solution under the given conditions. Any further improvement in the results if required would have to deal with the boundary conditions rather than the mesh parameters.

	Original Mesh	Coarse Mesh	Error	Refined Mesh	Error
T_o	38.6278	37.8643	1.98 %	38.6132	0.037 %
ΔP	3.921782	2.91701	25.62 %	3.9529011	0.780 %

Table 2   Comparison of original and refined meshes' results

CHAPTER 6

RESULTS AND DISCUSSION

6.1 SIMULATION RESULTS

Six different Reynolds numbers were investigated in all ribbed cases as well as the smooth case ranging from 2,000 to 20,000. These values were obtained from the experimental data by Al-Habeeb [5].

The following figures illustrate various aspects of the flow properties for the smooth case and sample of the ribbed cases. These aspects include pressure variation across the flow, temperature distribution and the velocity vectors.
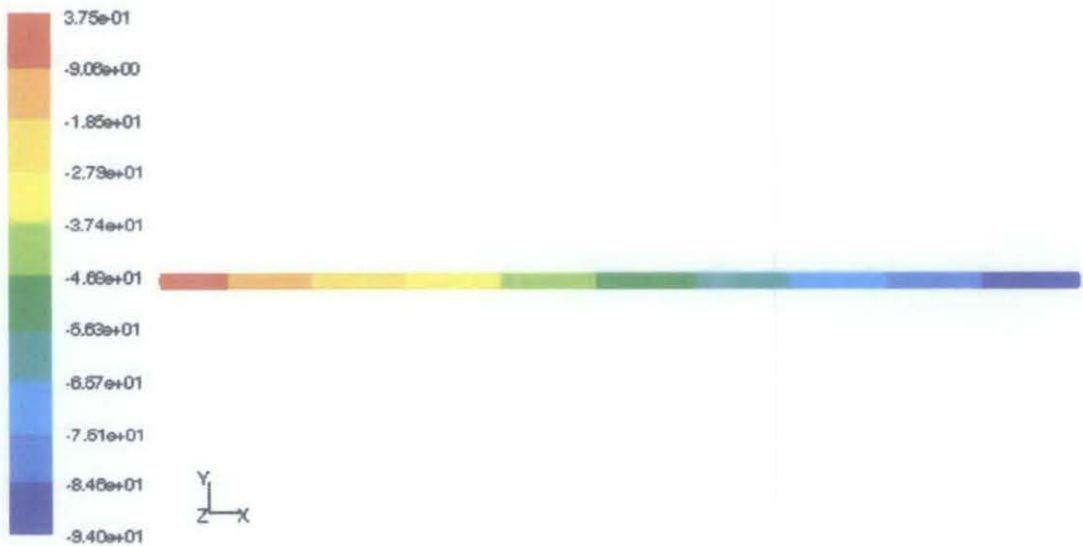
Figure 11   Static pressure profile for the smooth case

Figure 12   Temperature distribution for the smooth case
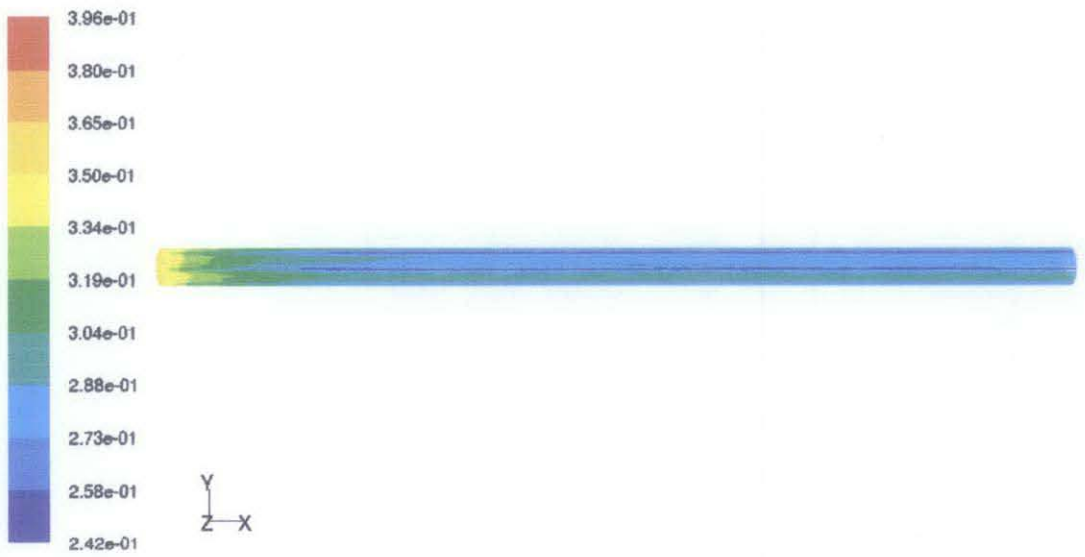
Figure 13   Velocity vectors for the smooth case

Figure 14   Sample pressure profile for ribbed cases

Figure 15   Sample temperature profile for ribbed cases
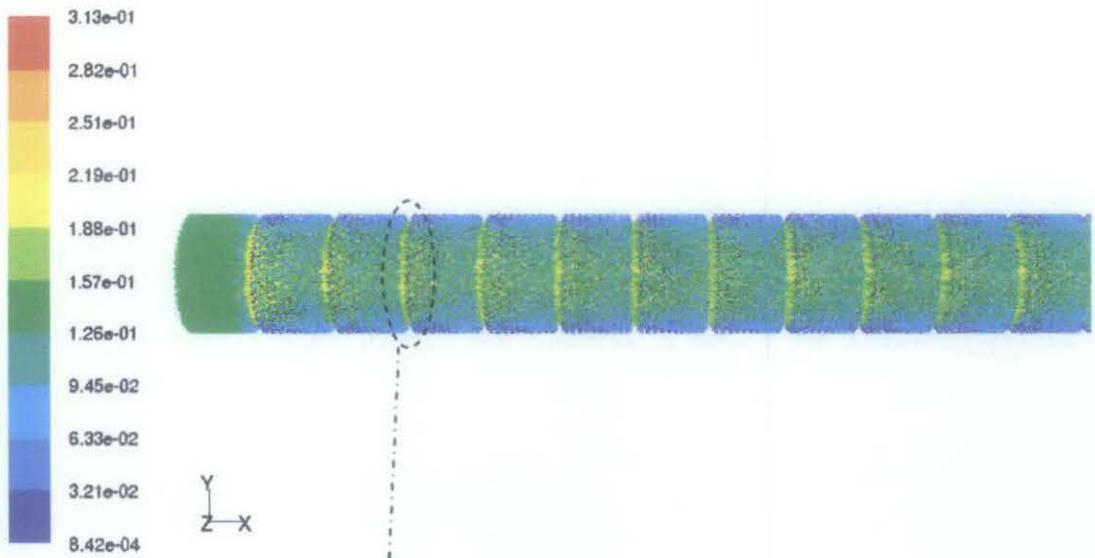
Figure 16   Sample velocity profile for ribbed cases

Figure 17   2D velocity profile near the ribs

The last two figures above illustrate the velocity vectors for the ribbed cases. It is noted that vortices are induced in the vicinity of the ribs. These vortices are the main ribbing effect on the flow, wherein their effect on other flow parameters can be seen as a consequence of the induced vortices. The vortices cause the fluid molecules to collide and hence enhance the heat transfer. On the other hand, these collisions obstruct the flow and hence increase the friction.

6.2   VALIDATION OF RESULTS

In this section, results from the two procedures are compared against experimental data for validation. Three different parameters are presented below. These are the outlet temperature, Stanton number and friction factor for smooth case ribbed cases. *(Detailed results are tabulated in appendix D)*
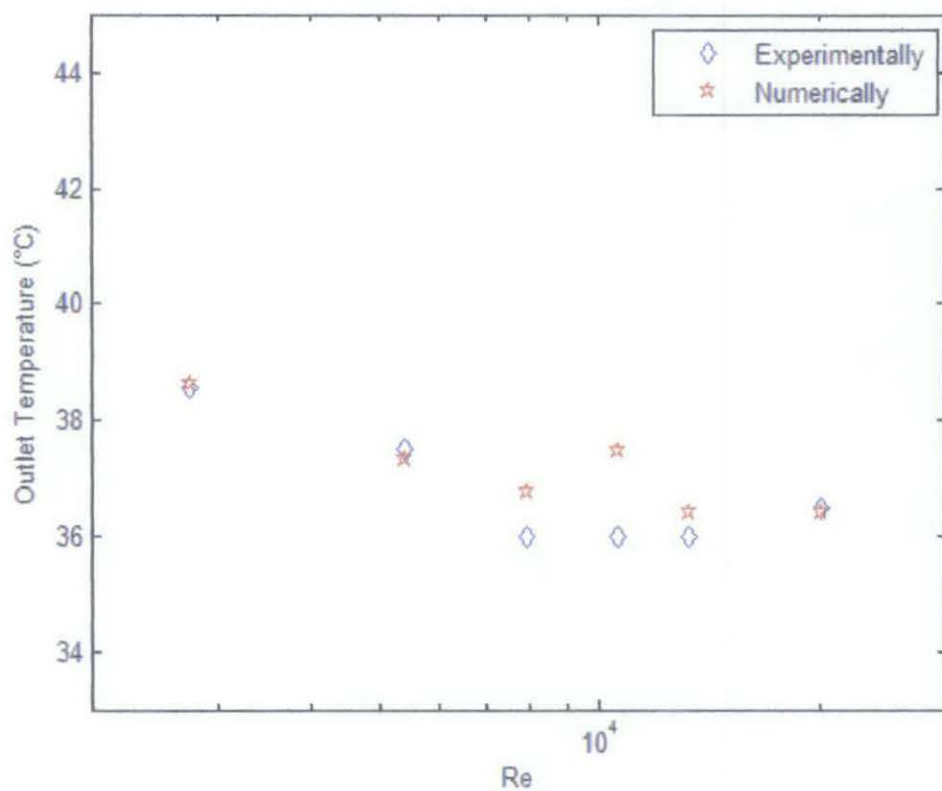
Figure 18   Outlet Temperature for Smooth Case
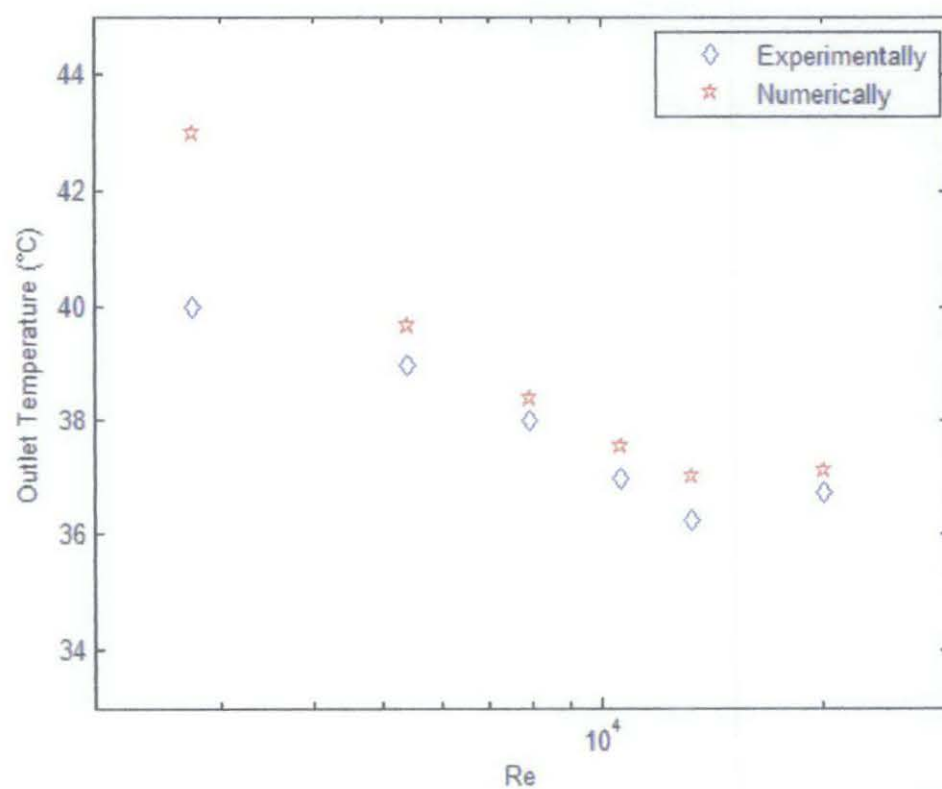
Figure 19   Outlet Temperature for Ribbed Case 1

28
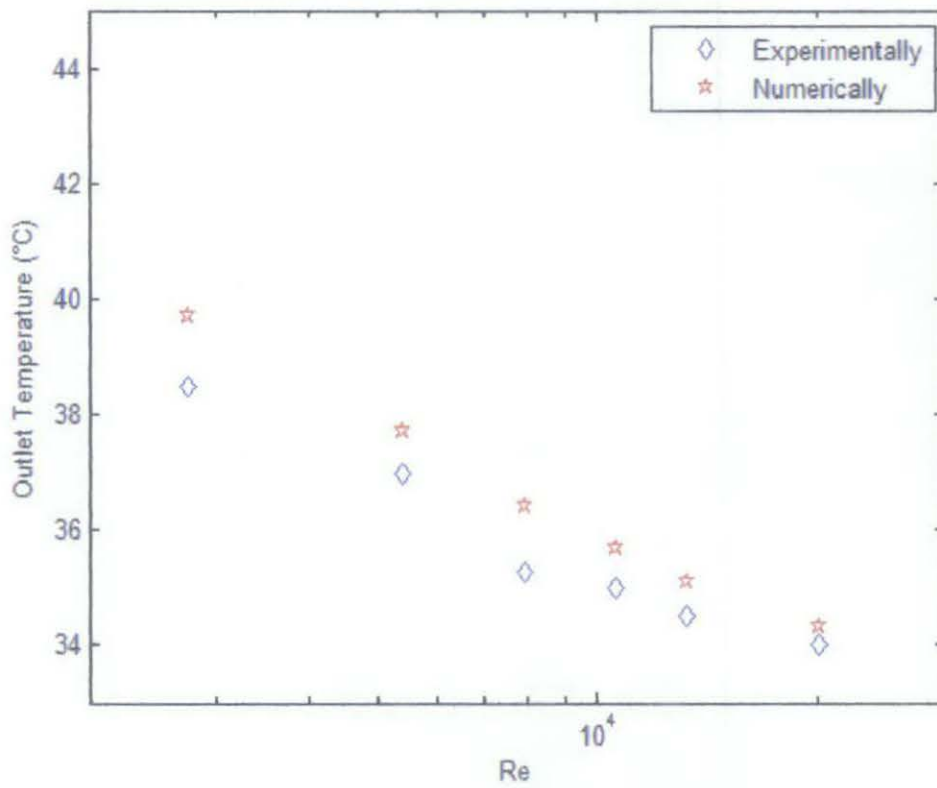
Figure 20   Outlet Temperature for Ribbed Case 2
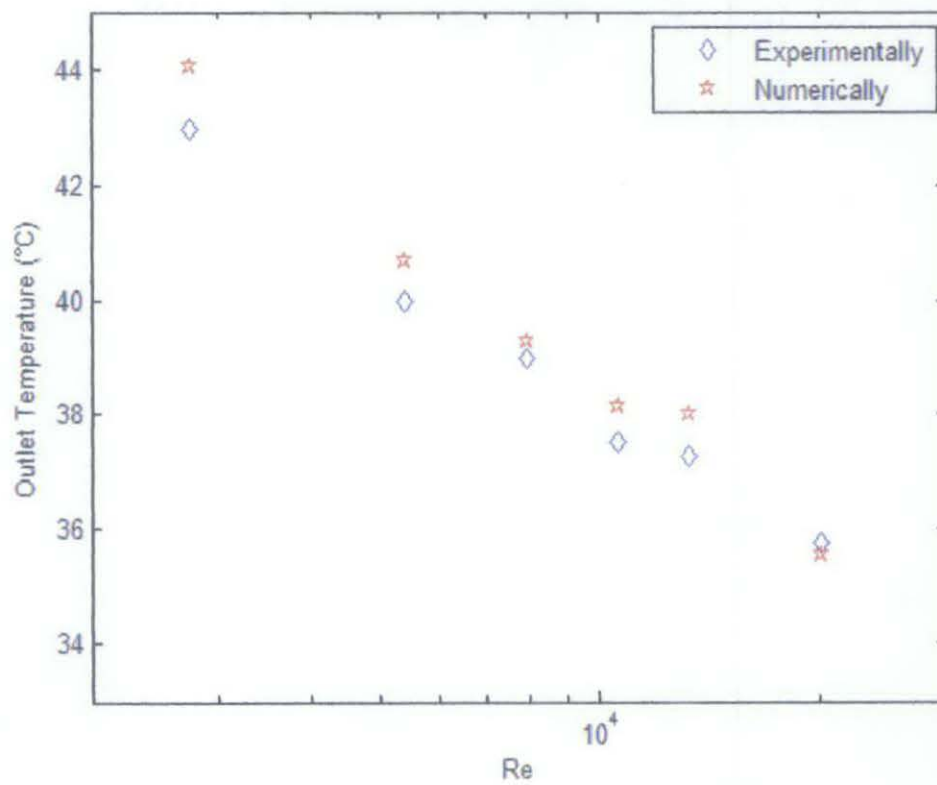
Figure 21   Outlet Temperature for Ribbed Case 3
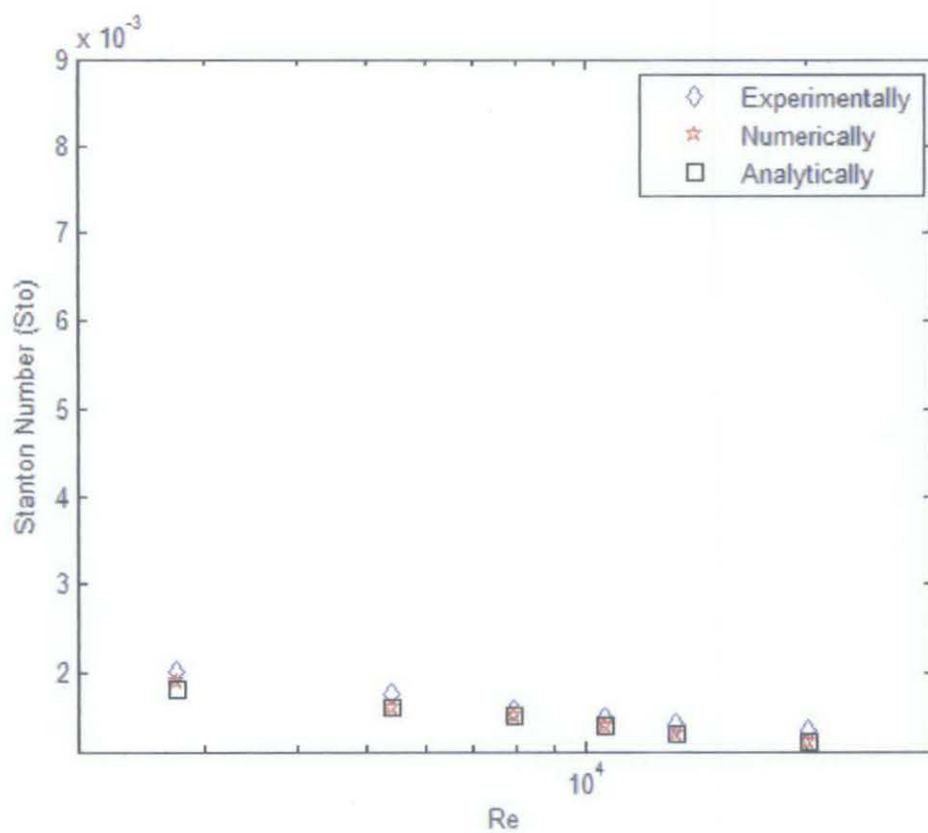
Figure 22   Stanton number Vs Re for smooth case
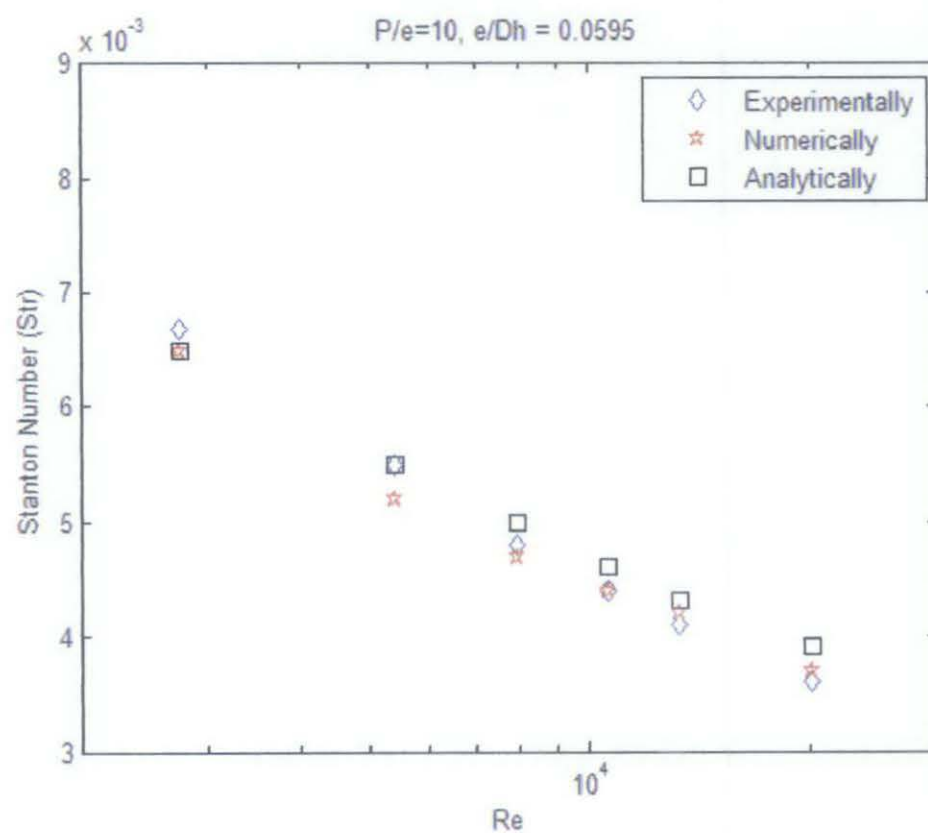
Figure 23   Stanton number Vs Reynolds number for ribbed case 1
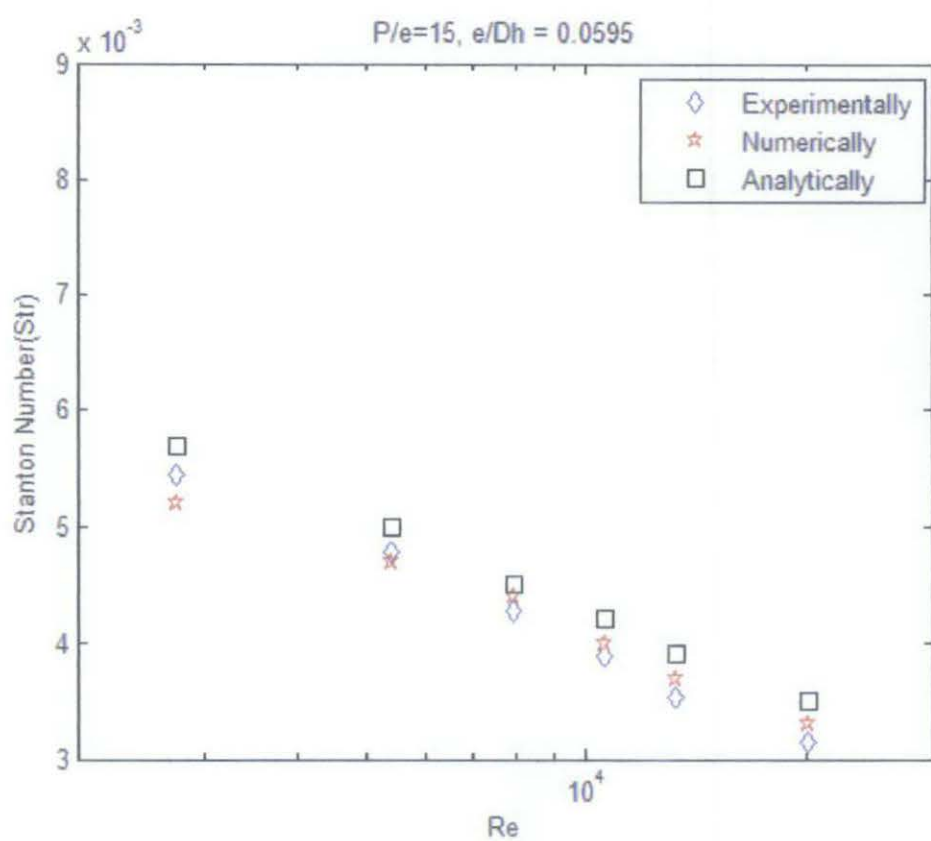
Figure 24   Stanton number Vs Reynolds number for ribbed case 2
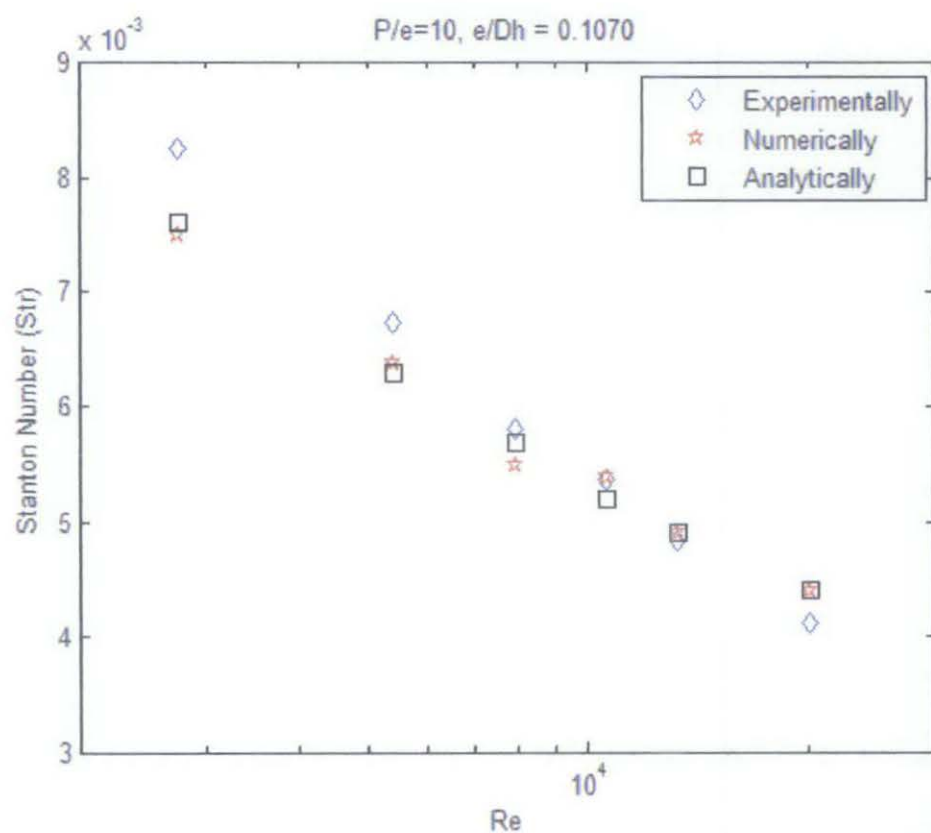
Figure 25   Stanton number Vs Reynolds number for ribbed case 3
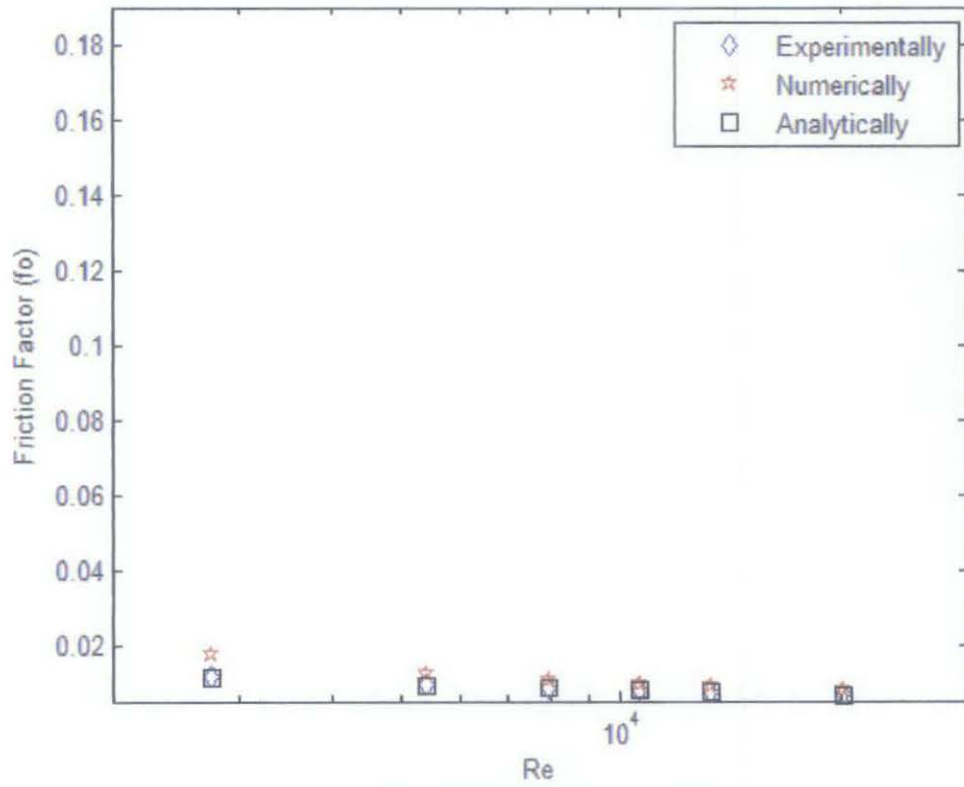
Figure 26   Friction factor Vs Re for smooth case

P/e=10, e/Dh = 0.0595
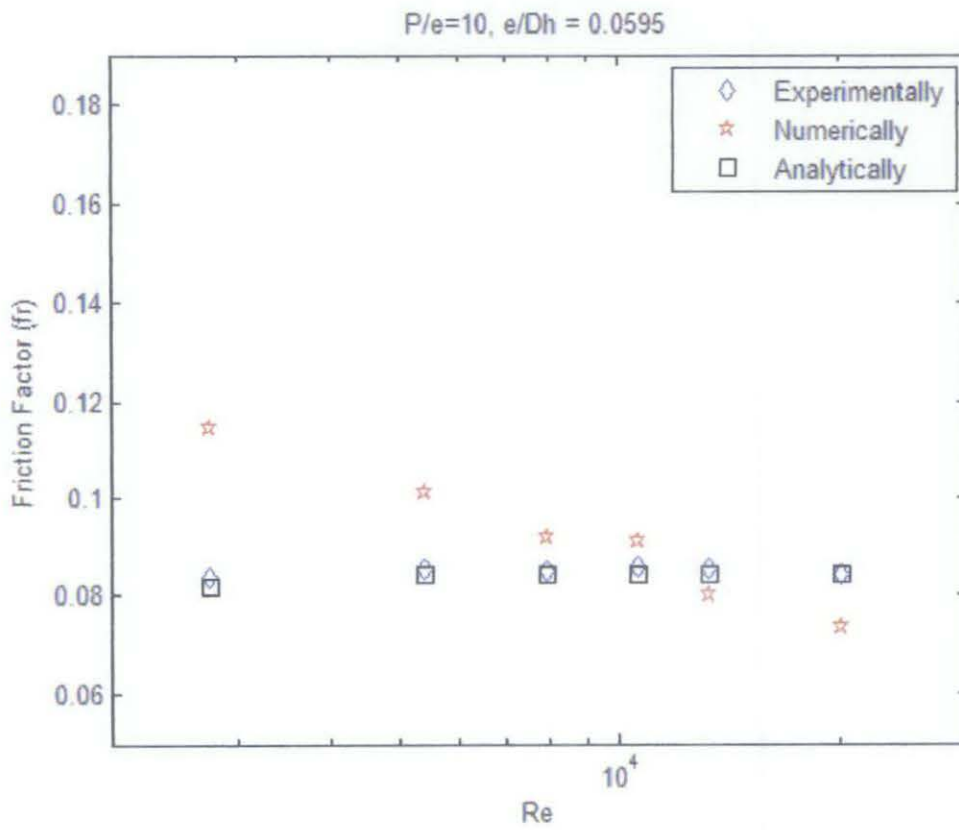
Figure 27   Friction Factor Vs Re for ribbed Case 1
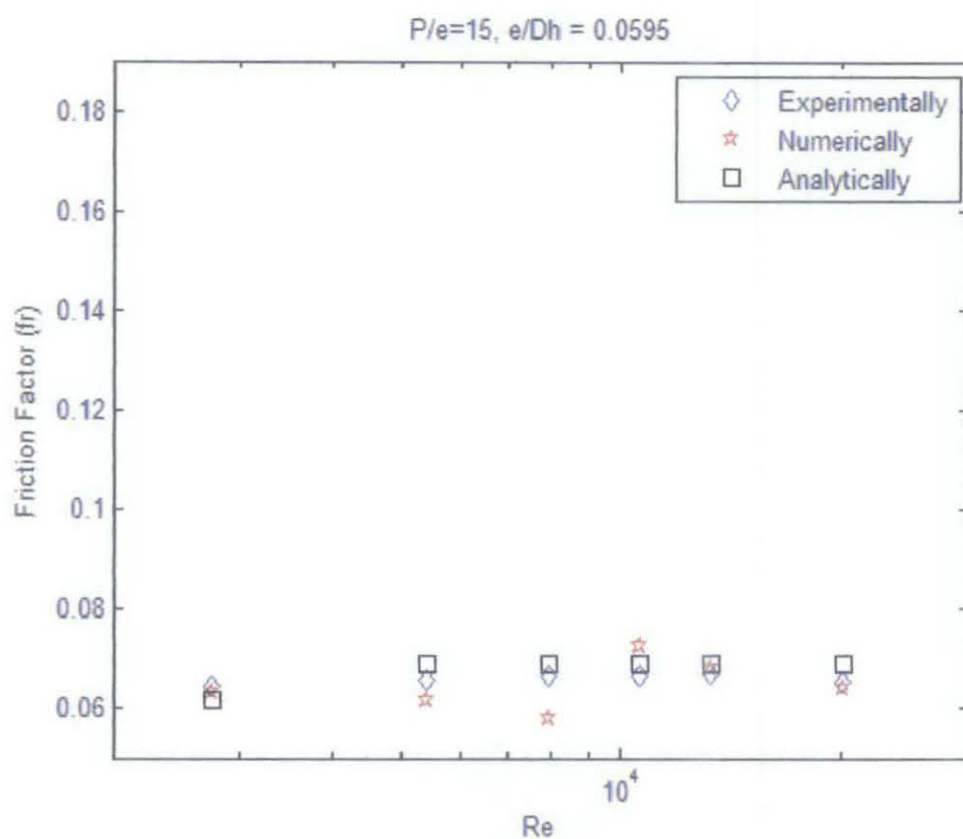
Figure 28   Friction Factor Vs Re for ribbed Case 2
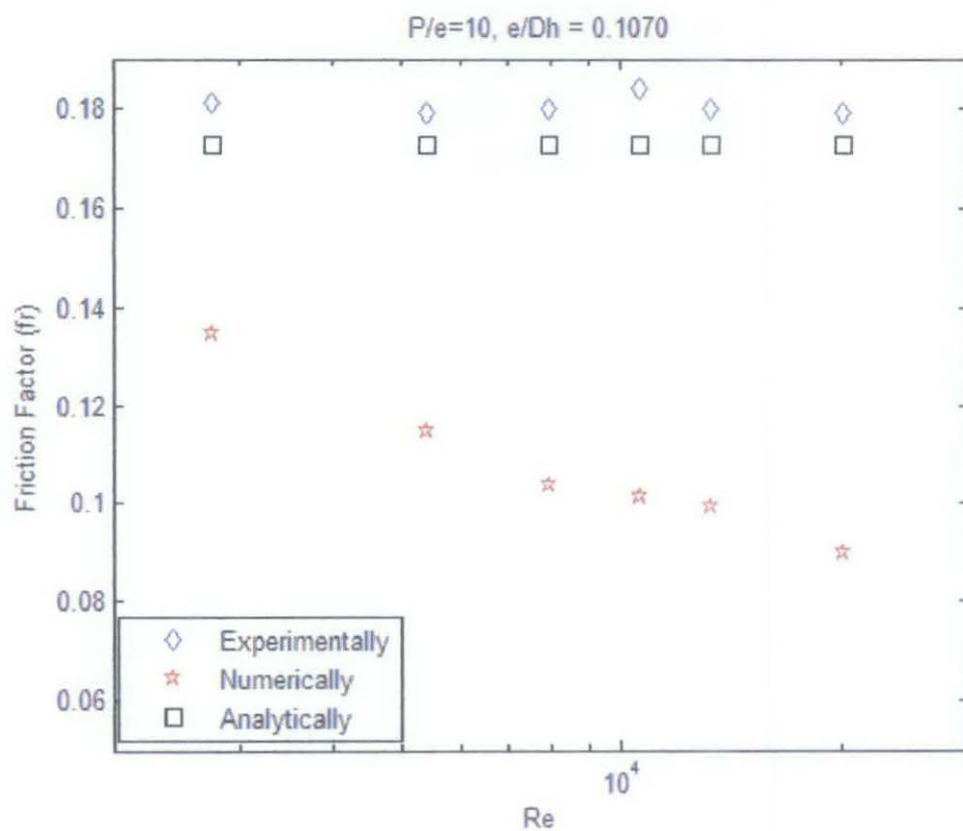
Figure 29   Friction Factor Vs Re for ribbed Case 3

33

The temperature results reveal good agreement between the numerical and the experimental data. This validates the thermal boundary condition assumption mentioned in section 5.3.1. It is noted however on the smooth case figure that greater discrepancy was sustained for the mid range values. The experimental data for this range showed constant value for the Reynolds numbers which is believed to be an error in reporting the experiment data where it is expected that temperature should vary as Reynolds number changes.

Stanton number which is a function of the outlet temperature showed good agreement too, both numerically and analytically. From these two remarks a conclusion is drawn that heat transfer was successfully modeled analytically and numerically.

Considering the friction factor for the smooth case, it is noted that generally Blasius correlation is more conservative than Mc Adams'. However Mc Adams' is closer to experimental results. The two correlations tend to become identical at high Reynolds numbers. For the ribbed cases, analytical results show good agreement with the experimental data which validates the used procedure to analytically model the friction factor. Numerical data on the other hand exhibit greater discrepancy specially for the third case. This may be attributed to errors in pressure conditions used during the simulation. However with the absence of the pressure data for the experiment it is not possible to confirm the source of discrepancy.

The general trend observed in both friction factor and Stanton number figure is that as Reynolds number increases, both friction factor and Stanton number decrease. The decrease in the friction factor can be explained by considering the fact that Reynolds number, of which both friction factor and Stanton number are functions, is the ratio of inertia forces to frictional forces expressed by the fluid viscosity. At high Reynolds numbers velocity increases and eventually, inertia forces outweigh frictional forces.

The following figures illustrate the relative increase in both Stanton number (heat transfer enhancement) and the friction factor which are the ratio of Stanton number and the friction factor for ribbed cases to the smooth case respectively. These two parameters are usually the main parameters of focus when assessing the ribbing effect rather than considering their absolute values. As can be seen, generally, both

34

techniques' results match the experimental ones. Moreover, the numerical results are even able to capture trends better than the analytical procedure. It is to be noted here that despite the discrepancy exhibited by the numerical values of friction factor, when normalized by the smooth case it is able to give good match to the experimental results. This means that the numerical procedure can still be used to estimate the friction factor specially when used in combination with the analytical procedure.
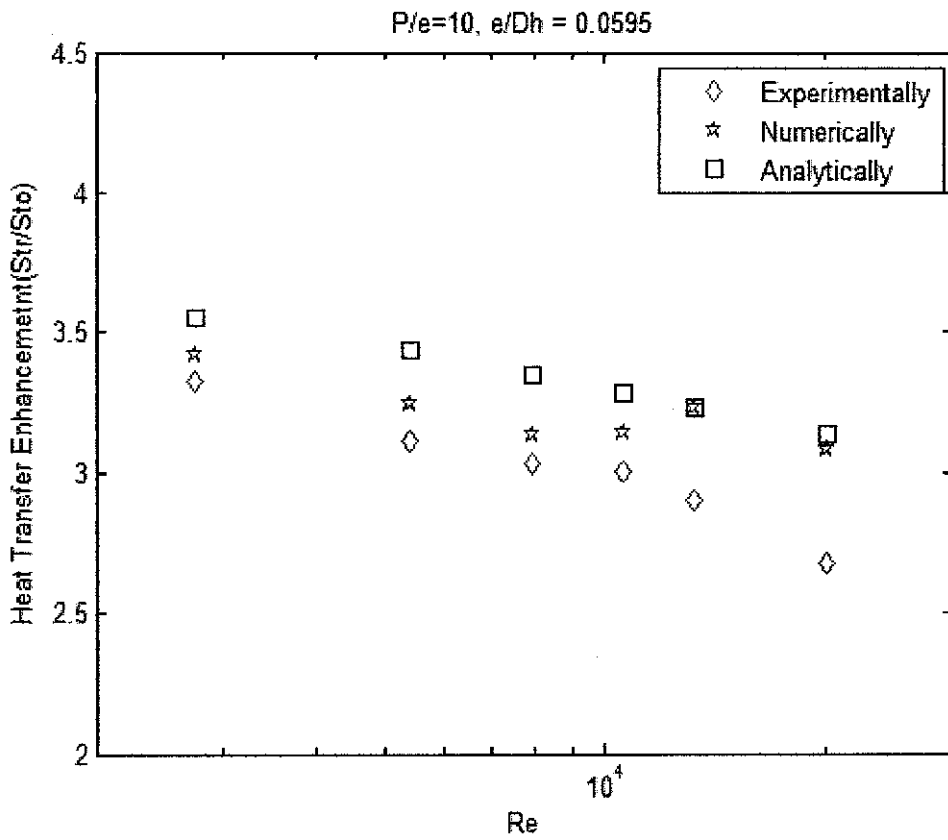
Figure 30   Heat transfer Enhancement for case1
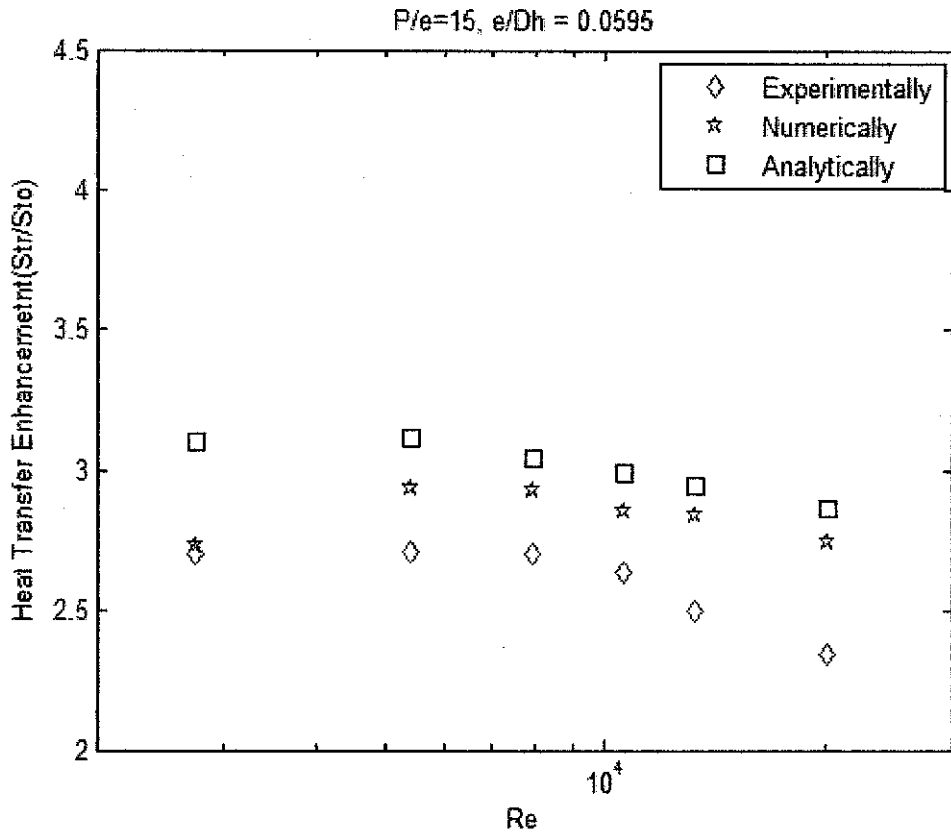
Figure 31   Heat transfer Enhancement for case2
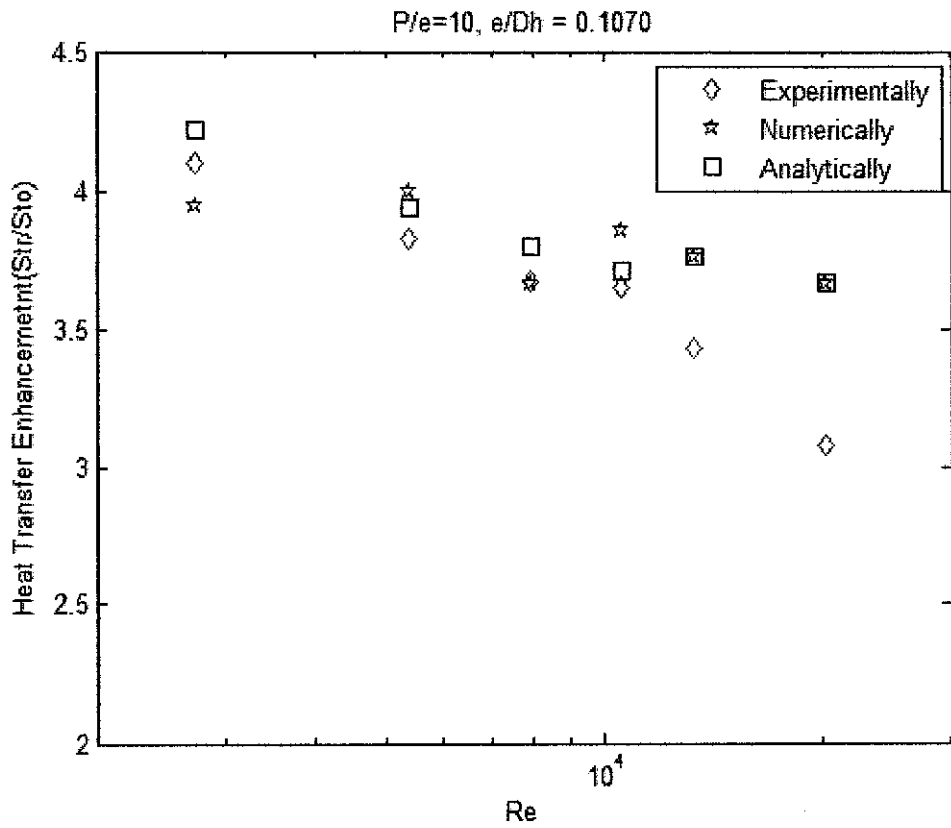
Figure 32   Heat transfer Enhancement for case1
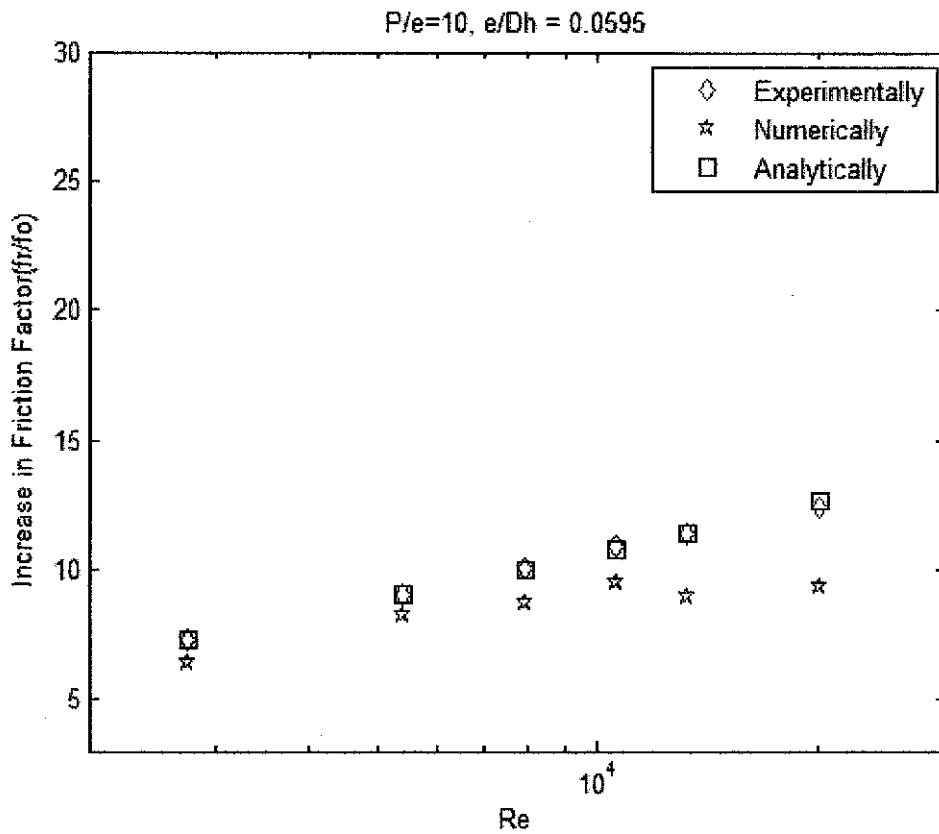
Figure 33   Relative Increase on Friction Factor for case1
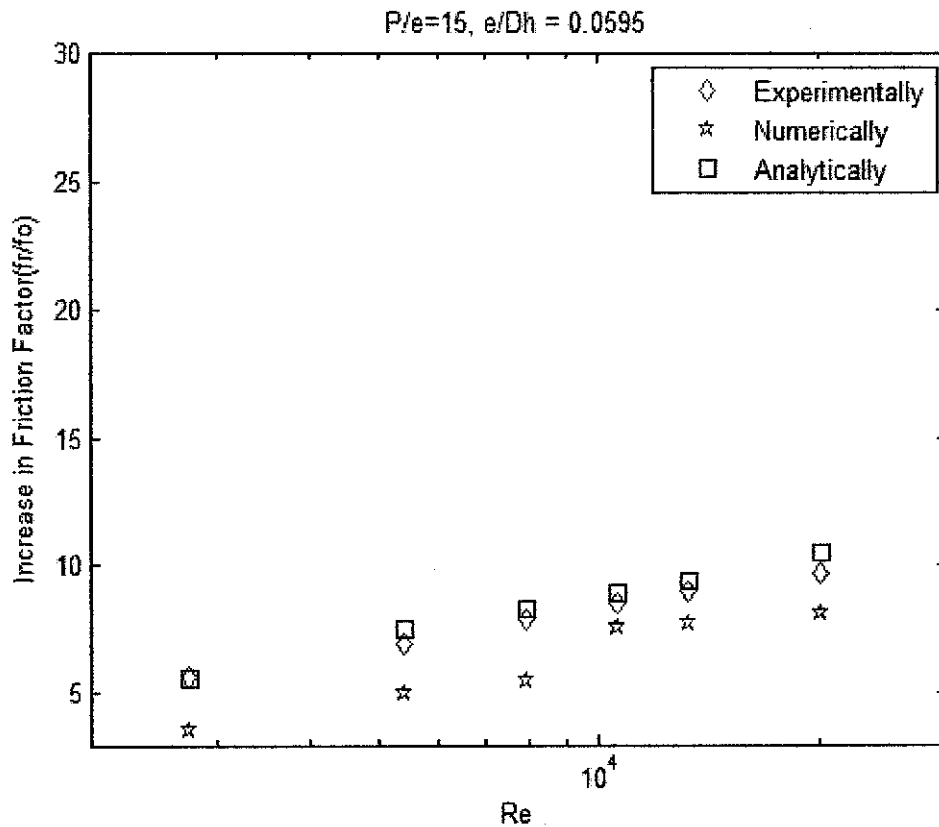
Figure 34   Relative Increase on Friction Factor for case2
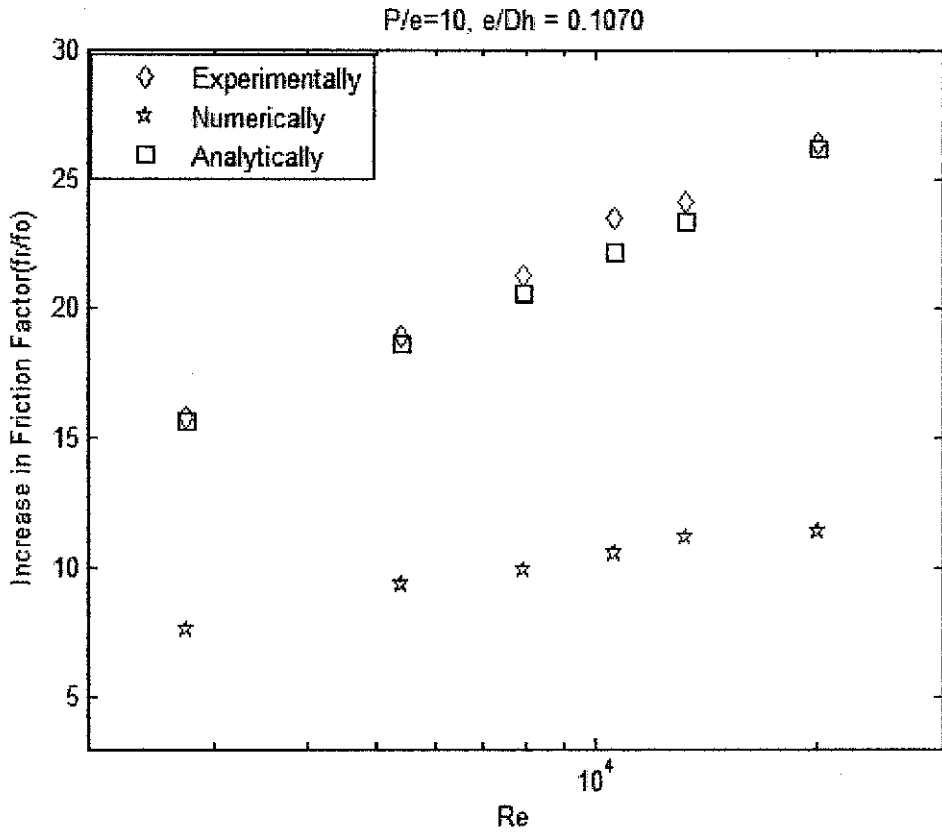
Figure 35   Relative Increase on Friction Factor for case3

In the following sections, light is shed on the effect of various ribbing configurations on the performance of the heat exchanger beginning with the effect of rib height (e). Results of the analytical procedure are used to plot the figures unless otherwise stated the analytical procedure was run on the entire range of Reynolds number permitted by the MC Adams and Blasisu Correlations (4,000 to 100,000)

6.3   EFFECT OF RIB HEIGHT
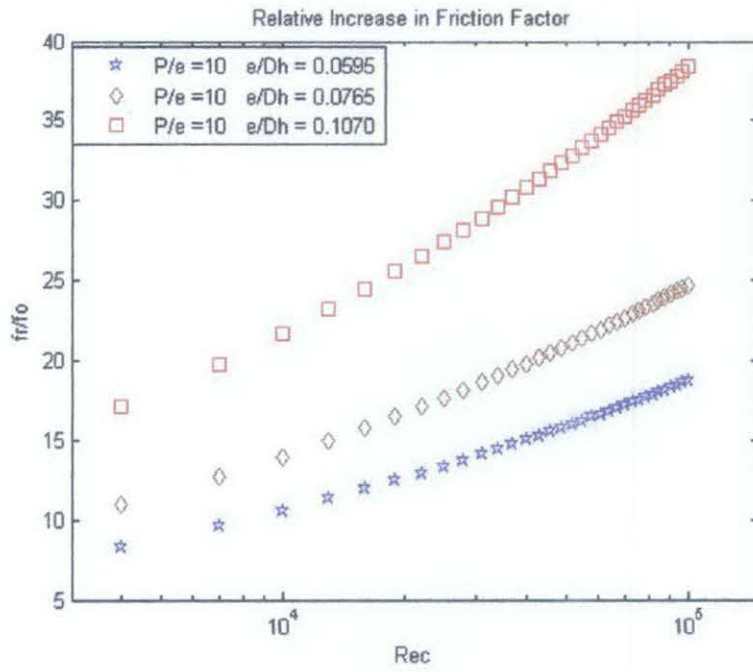
Figure 36   Relative Changes in Friction Factor (fr/fo) Vs Reynolds Number
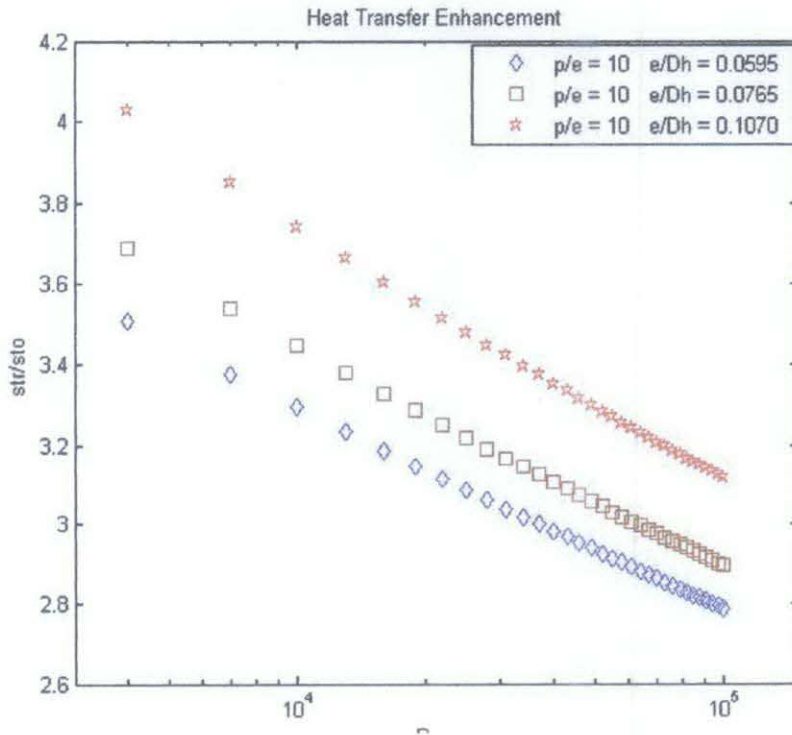
Figure 37   Heat Transfer enhancement (str/sto) Vs Reynolds Number

As reported by previous works in the literature, the heat transfer enhancement by the use of the ribs is accompanied by increasing pressure drop. Figure 36 above indicates

that the increase of friction factor and hence pressure drop are higher at high Reynolds numbers. It also indicates that as the rib height increases, so does the increase in pressure drop.

Heat transfer enhancement exhibits an opposite trend where the heat transfer enhancement drops as Reynolds number increases. Yet the trend with rib is similar. That is, as the rib height increases, the heat transfer increases as well. The following table shows the range of heat transfer enhancement along with the range of pressure drop for different rib heights at P/e=10.

e/D_h	St_r/St_o range		f_r/f_o range	
	From	To	From	to
0.0595	2.7873	3.5080	8.366	18.747
0.0765	2.8949	3.6892	11.026	24.708
0.1070	3.1173	4.0270	17.127	38.381

Table 3   Range of heat transfer enhancement and the corresponding increase in pressure drop

The following figures show the vortices generated by two ribs (e/D_h = 0.0595, 0.0765). The figures show that higher ribs result in larger vortices and more disturbances to the flow where it takes longer distance to resettle. This larger disturbance is the main cause of the increased friction.
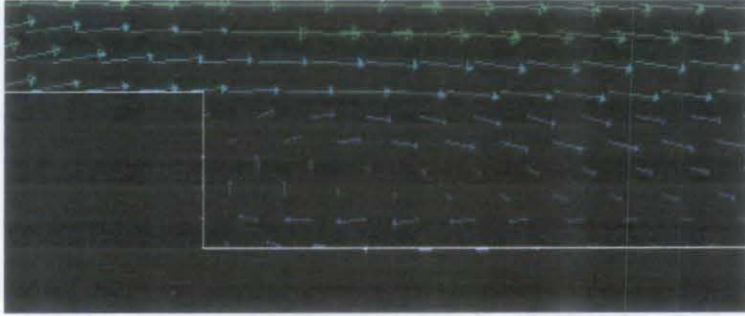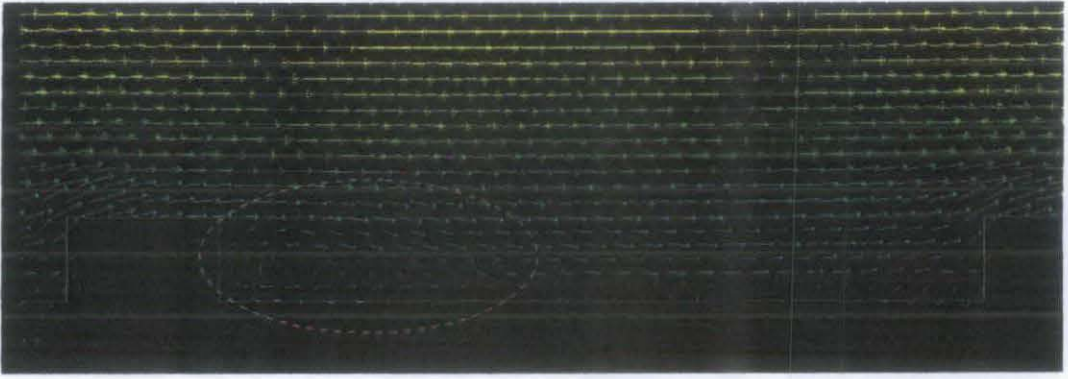
Figure 38   Vortices generated by rib with e=0.0595
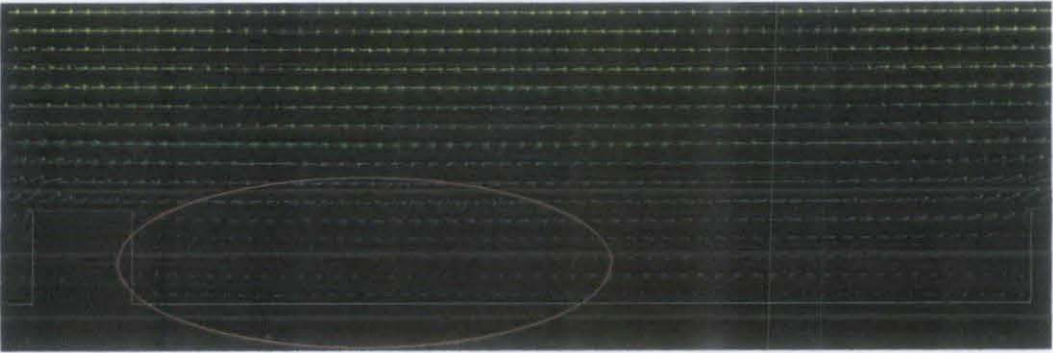
Figure 39   Vortices generated by rib with e=0.765

6.4 EFFECT OF PITCH DISTANCE

The second important parameter of focus in the analysis of ribbing effect is the pitch distance. This is the distance between the beginnings of any two consecutive ribs. The following figures illustrate the heat transfer and pressure drop behavior at different pitch sizes.
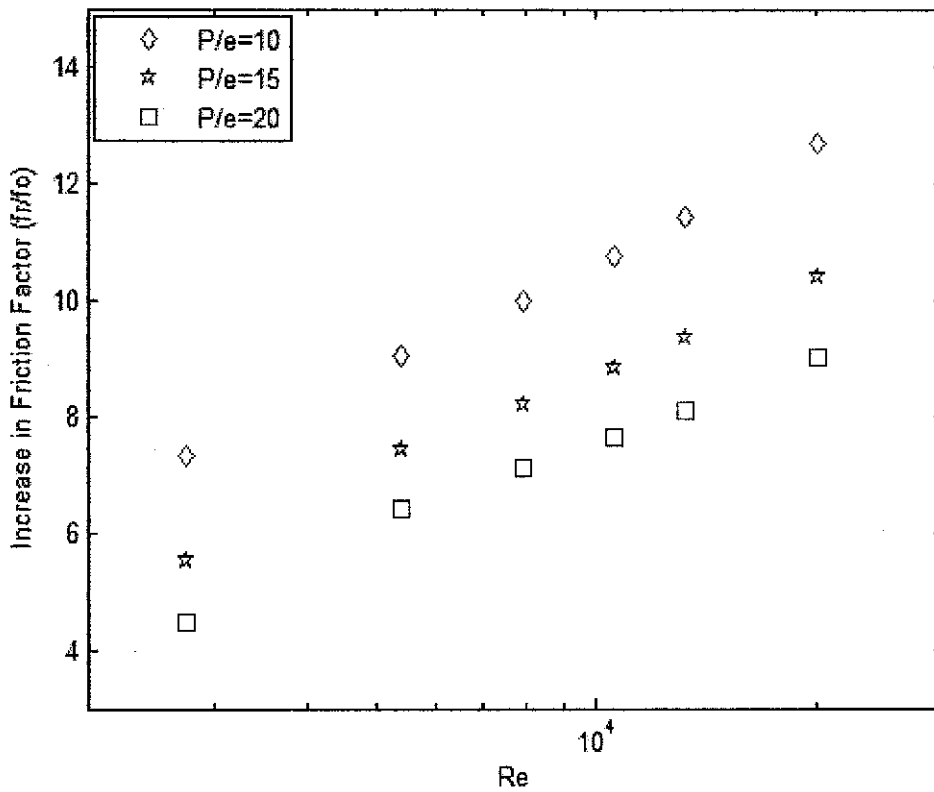
Figure 40   Relative increase in friction factor for three different pitch sizes
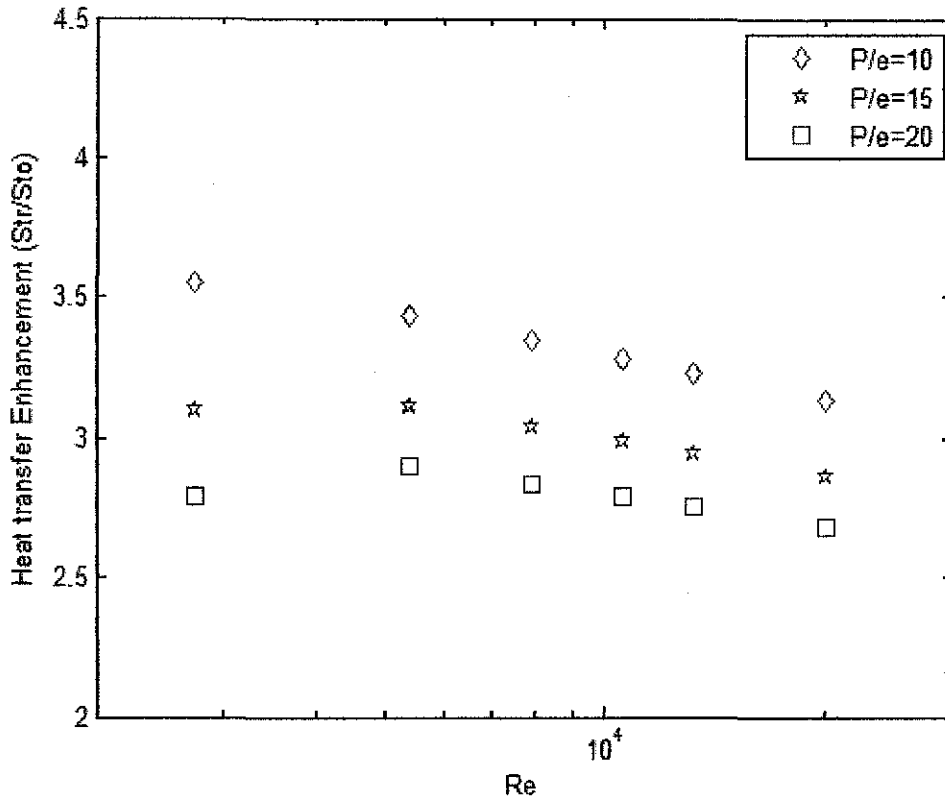
Figure 41   Heat transfer enhancement for three different pitch sizes

The observed trends from the previous figures show that increasing the pitch size decreases both the relative increase of friction factor and heat transfer enhancement. This is attributed to the fact that when the pitch distance increases, flow re-attachment to the surface increases and vortices induced by the ribs tend to settle. While at small pitches, re-attachment is less and vortices' wake is still active. This results in increasing the pressure drop and enhancing the heat transfer. This result is in line with the main objective of ribbing which is to induce vortices and turbulate the flow. The following figures compare the velocity vectors at the vicinity of the ribs for two different pitches (P/e = 10, P/e = 15). It is seen in the figures that flow settlement is better at higher pitches where it is completely settled well before reaching the following rib on the contrary to the case of smaller pitches.

Figure 42   Vortices generated at P/e-10
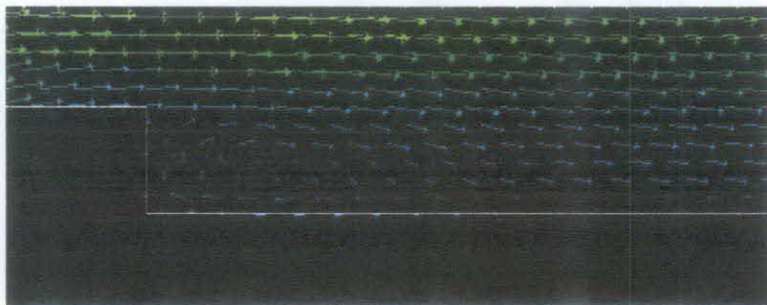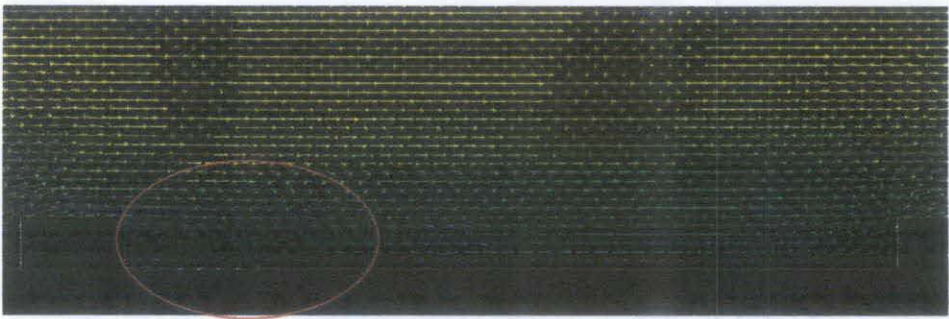
Figure 43   Vortices generated at P/e-15

6.5 ANNULUS EFFICIENCY INDEX η

The effect of both rib height and pitch distance was studied on the heat transfer and pressure drop separately. Various trends were observed for each parameter resulting from various aspects of the rib configuration (rib height and pitch). These various trends pose the need of having a tool which allows studying the effect all ribbing configurations on both heat transfer and pressure drop simultaneously. This tool, the annulus efficiency index η, was introduced by Webb [2] and it is defined as the amount of pressure drop which must be sacrificed in order to achieve a given amount of heat transfer enhancement. In mathematical form, it is the ratio of heat transfer enhancement to the relative increase in friction factor:

$$\eta = \frac{Str/Sto}{fr/fo} \qquad (22)$$

The following figures show the efficiency index for different configurations. First, the index is evaluated for cases 1, 2, 3 both analytically and numerically and compared with the corresponding experimental data (these figures show the index at a single ribbing case). Later, the index is evaluated analytically for all ribbing configurations which are combined in one figure.

45
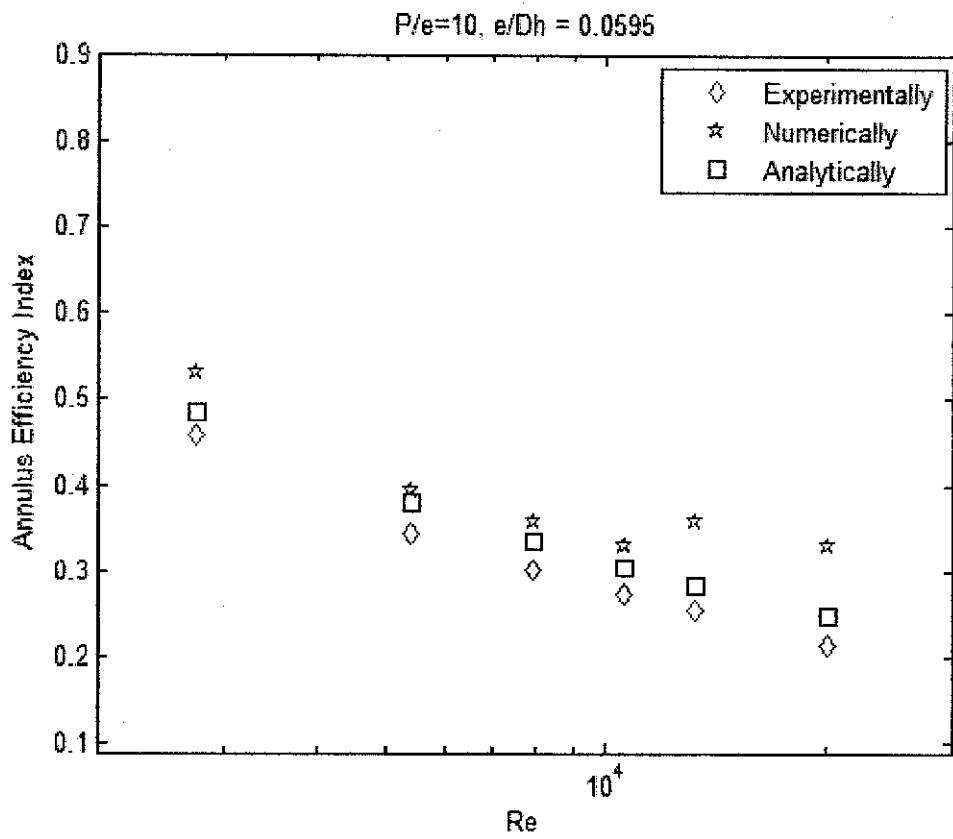
Figure 44   Annulus efficiency index for ribbed case 1
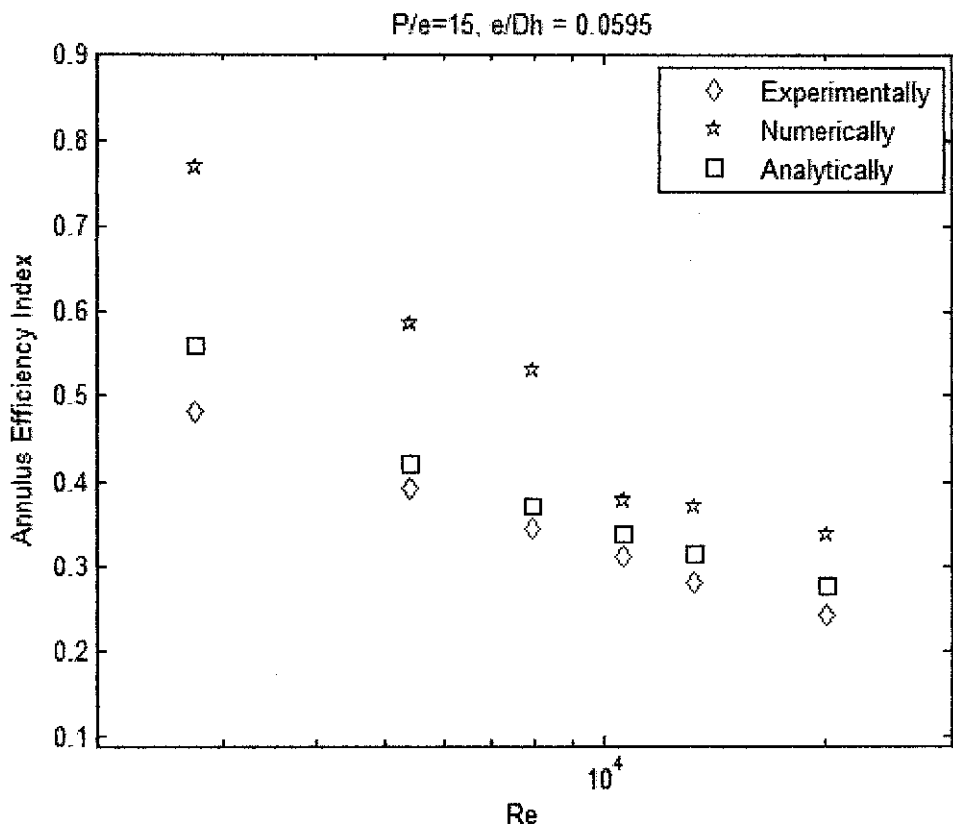
Figure 45   Annulus efficiency index for ribbed case 2
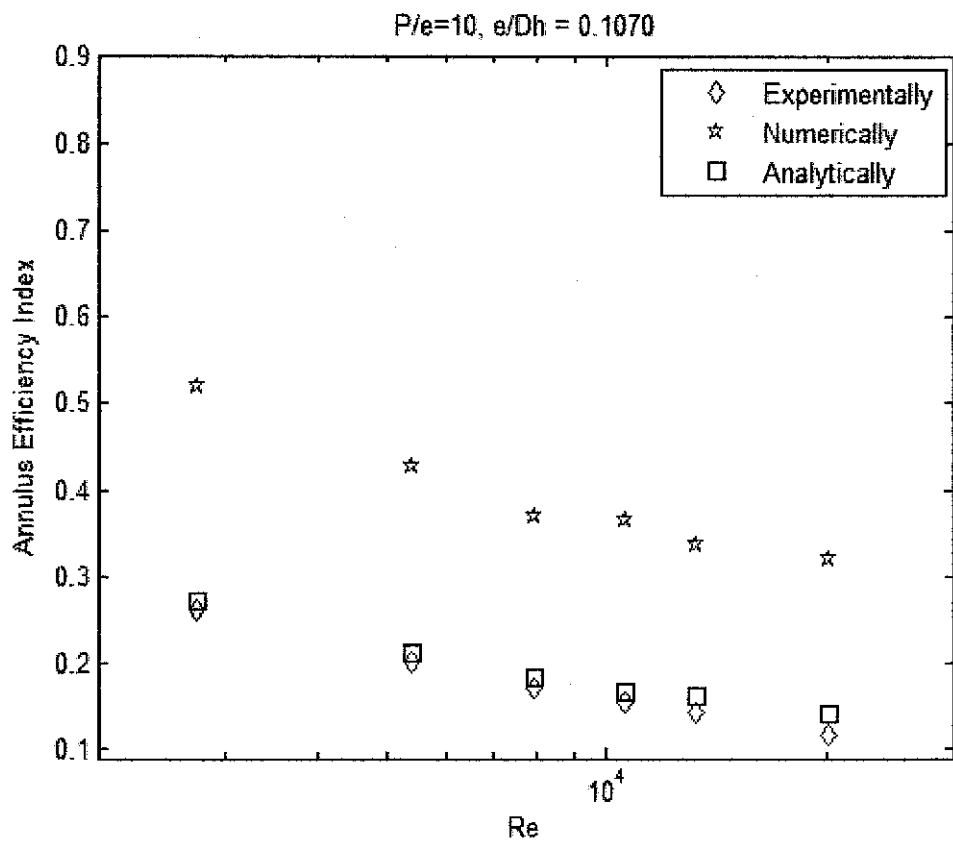
Figure 46 Annulus efficiency index for ribbed case 3
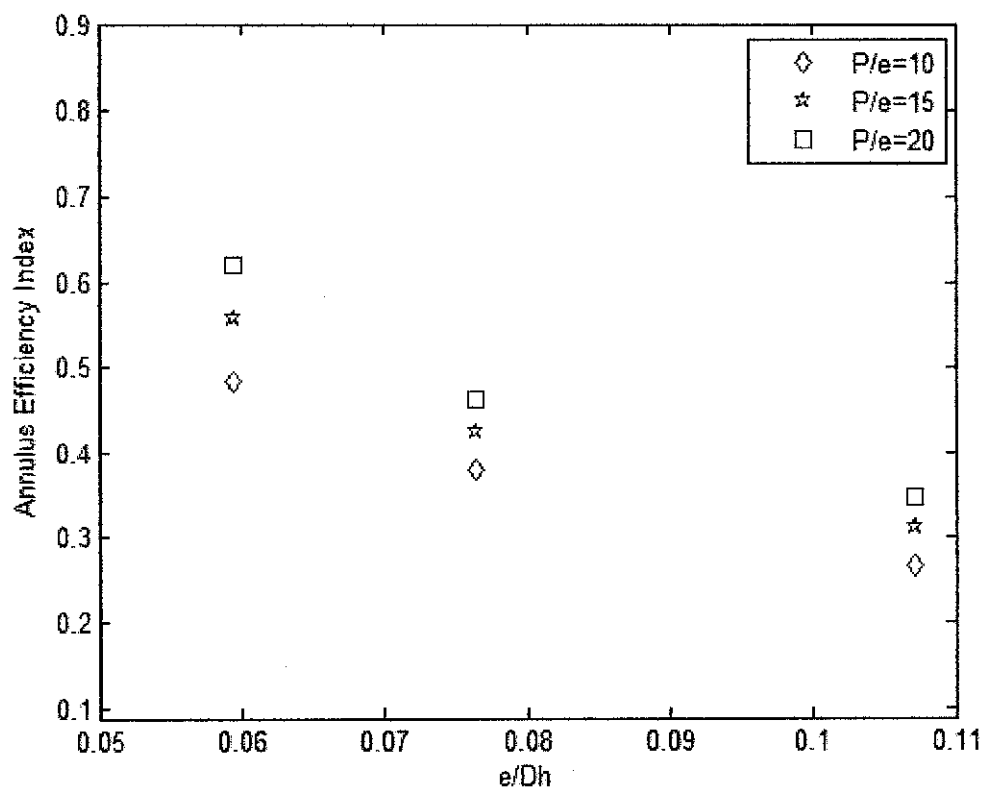
Figure 47   Annulus Efficiency index (η) Vs rib height for different pitch sizes

The three comparison figures show that the analytical procedure gives excellent estimate of the efficiency index for all cases. Numerical procedure too gives good estimates of the index yet, discrepancies do occur for some cases. The discrepancy source is due to the inherent error in estimating the friction factor as seen earlier.

A main observation regarding the efficiency index is that it assumes values less than 1 all the time which indicates that the accompanying pressure drop outweighs the heat transfer enhancement. Two more trends are observed in figure 42: first, increasing the rib height results in decreasing the efficiency index. Second, as the pitch distance increases, so does the efficiency index. The first trend implies that increasing the rib height contributes more friction with decrease heat transfer enhancement which explains the declining trend. The later implies that allowing the flow to reattach to the surface before re-inducing the vortices yields better enhancement in heat transfer than continuously inducing the vortices in the wake of their predecessors this also explain the trends seen in section 5.4 where increasing the pitch distance results in less pressure drop while it better enhances heat transfer.

Plotting a figure similar to figure 40 above on a wide range of pitches and rib heights allows designers to optimize the ribbing configuration to match the available pumping power with the desired heat transfer enhancement.

A final remark regarding the efficiency index is that it should not be miss interpreted. That is, having low efficiency does not necessarily imply a low gain (heat transfer enhancement). It may be due to losses (pressure drop) much greater than the gain (e.g. efficiency of 0.5 may be a result of a ratio of 5/10 or 10/20. In the latter case, more heat transfer enhancement is achieved which in some cases could be attractive despite the 20 times pressure drop).

6.6   RIBS ON THE INNER PIPE

All the previous discussion was based on the case of ribs installed on the annulus. In this section the effect of ribbing the inner pipe instead is discussed. The case of ribs on the inner pipe was studied numerically and compared with a similar annulus ribbing case (same e, P, and inlet parameters). The following figures compare the

outlet temperature, Stanton number and the friction factor of the two cases. (i.e. ribs on the annulus and on the inner pipe).
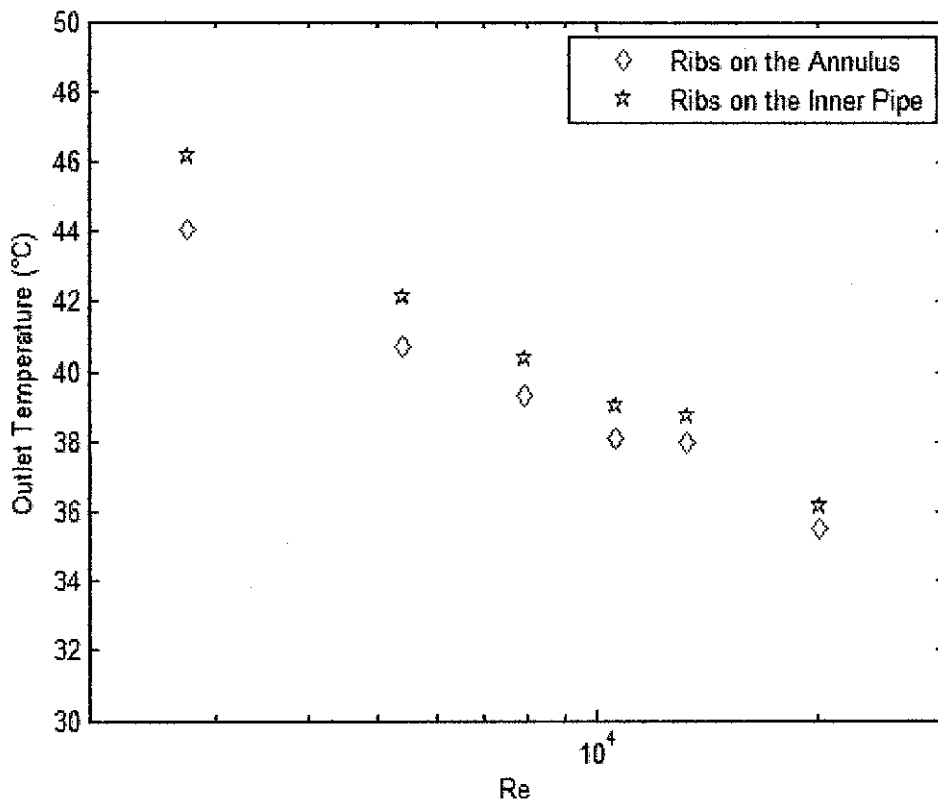
Figure 48   Outlet Temperature Vs Reynolds number
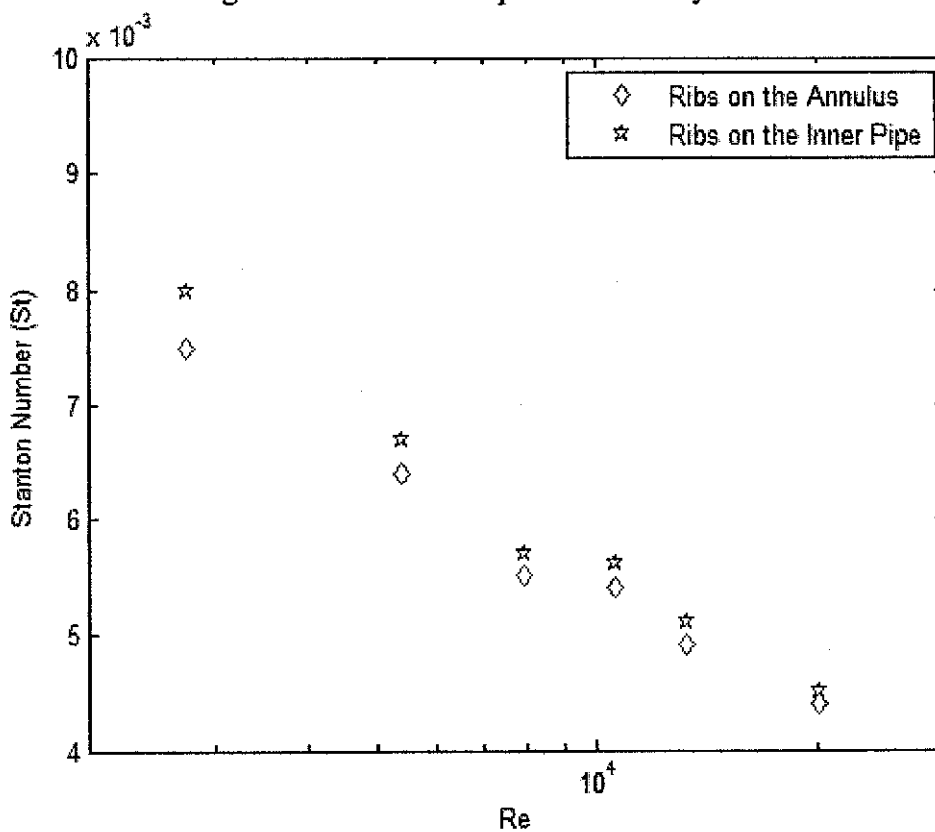
Figure 49   Stanton number Vs Reynolds number
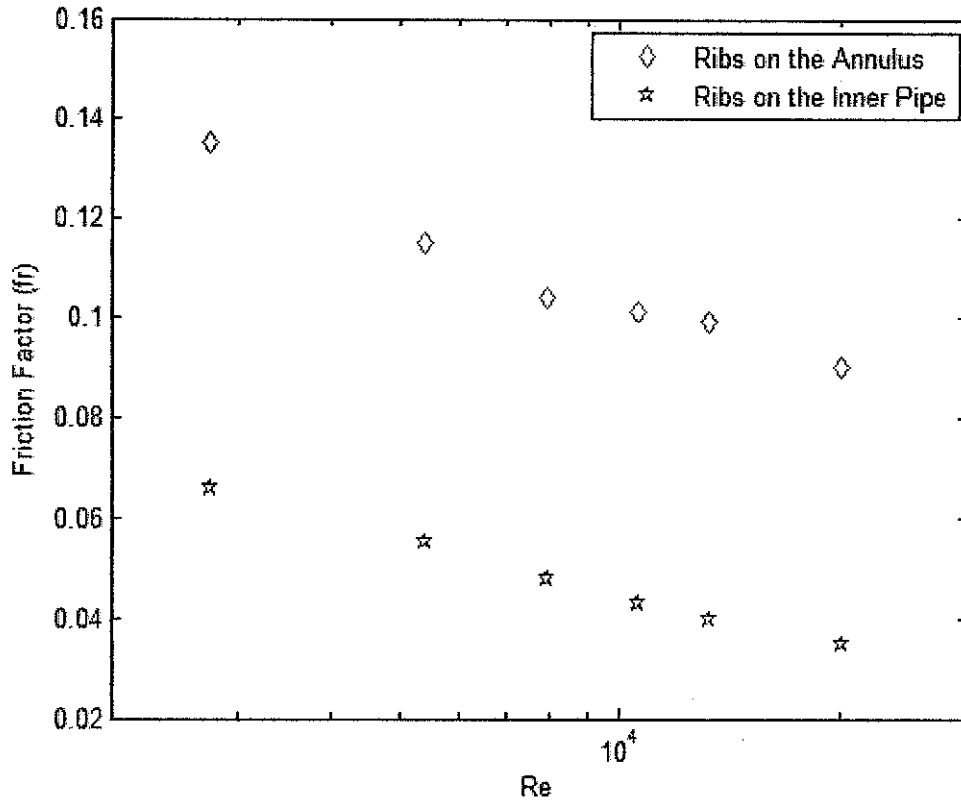
Figure 50   Friction factor Vs Reynolds number

The temperature figure shows that higher temperatures are obtained when ribs are on the inner pipe. Stanton number too, attains higher values in the case of ribs on the inner pipe. These observations follow logically considering the fact that heat transfer takes place on the surface of the inner pipe. Installing ribs on that surface extends the heat transfer area and at the same time induces turbulence in the flow and hence, the ribs contribute to heat transfer in two ways.

The friction factor when ribs are on the annulus is much greater than for ribs on the inner pipe (almost twice). The outer diameter of the inner pipe is 38mm and the annulus diameter is 76mm which is exactly double the inner pipe and therefore, annulus ribs are also double the size of the inner pipe ribs. Vortices generated on the annulus are generated on a larger diameter than those on the inner pipe. Hence they result in more friction than their counter vortices generated on the inner pipe.

The previous figures show that ribbing the inner pipe results in greater heat transfer and less friction. Consequently, it is expected that the efficiency index is greater than the annulus ribbing case. It should be noted however that the improved efficiency

50

index for the inner pipe ribbing is attributed mainly to the decreased friction in the flow compared to the case of annulus ribbing. The efficiency index of the two cases is plotted over the Reynolds number range in the following figure.
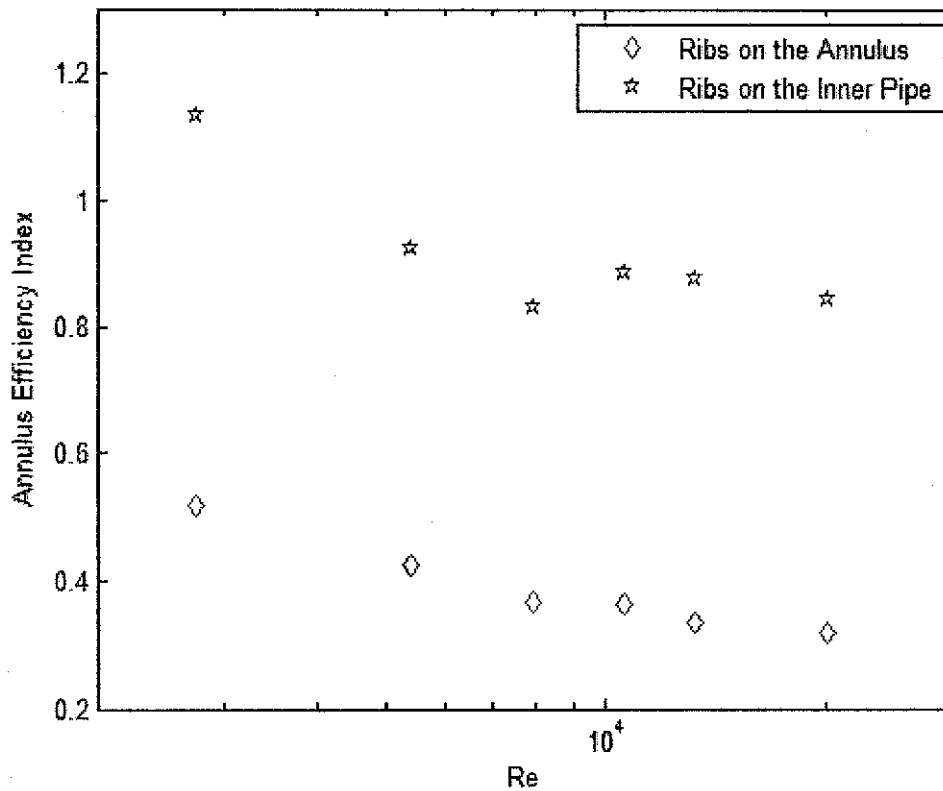
Figure 51   Annulus efficiency index Vs Reynolds number

Chapter 7

CONCLUSIONS AND RECOMMENDATIONS

7.1 CONCLUSIONS

The flow in a ribbed double pipe heat exchanger was modeled both analytically and numerically on Reynolds number ranging from 2000 to 20,0000. The analytical analysis is based on empirical equations and correlations introduced by previous researchers in the field while the numerical analysis employed a commercially available CFD code, FLUENT, to simulate the flow and evaluate its main properties such as velocity, pressure and temperature.

Different ribbing configurations including various rib heights, pitch distances and ribbing on the inner pipe were studied. The main parameters of focus are the heat transfer enhancement expressed by Stanton number and the pressure drop expressed by the friction factor.

The thermo fluid mechanisms governing the flow phenomena were studied based on the obtained results to develop a generalized understanding of the heat transfer and pressure drop behavior.

Ribbing was found to enhance the heat transfer by more than 3 times at an expense of increasing pressure drop of more than 18 times. Ribbing on the inner pipe instead of the outer pipe was found to yield better enhancement of heat transfer and less friction losses.

7.2 RECOMMENDATIONS

Several other parameters need to be considered to come into full understanding of the heat transfer and pressure drop with the presence of ribs, these parameters include:

1- To investigate the effect of the angle of attack on the performance of the heat exchanger.

2- To investigate the effect of the shape angle on the performance of the heat exchanger.

3- To investigate the phenomena on rectangular cross sections.

REFERENCES

[1] Nikuradse, J., "Laws for Flow in Rough Pipes", VDI Forsch.361, series B, 4 NACA YM, 1950

[2] Webb, R. L., Eckert, E. R. G. And Goldstein, R. J., "Heat Transfer and Friction in Tubes with Repeated-Rib Roughness", Int. J. Heat Mass Transfer, Vol. 14, pp. 601-617, 1970

[3,a] Kazuyuki Takase, "Experimental Results of Heat Transfer Coefficients and Friction Factors in a 2D / 3D Rib-Roughened Annulus",

[3,b] Kazuyuki Takase, "Numerical Prediction of Augmented Turbulent Heat Transfer in an Annular fuel Channel with Repeated Two-Dimensional Square Ribs", Nuclear Engineering and Design 165 (1996) 225 237

[4] Cengiz Yildiz, Yasar Bicer and Dursun Pehlivan, "Effect of Twisted Strips on Heat Transfer and Pressure Drop in Heat Exchangers", Energy Convers, Mgmt Vol. 39, No. 3/4, pp. 331-336, 1998.

[5] H. Braun, H. Neumann, N.K. Mitra, "Experimental and Numerical Investigation of Turbulent Heat Transfer in A Channel with Periodically Arranged Rib Roughness Elements", Experimental Thermal and Fluid Science 19 (1999) 67±76.

[6] Laheeb, A.-H. N. (1999). Performance Enhancement of Double Pipe Heat Exchangers by Enforced Turbulence on Single Surface. Baghdad.

[7] Hacı Mehmet Sahin, Ali Rıza Dal, Esref Baysal, "3-D Numerical Study On The Correlation Between Variable Inclined Fin Angles And Thermal Behavior In Plate Fin-Tube Heat Exchanger", Applied Thermal Engineering 27 (2007) 1806–1816.

[8] Al-Kayiem,H.H, Al-Habeeb,L.N, "Performance Enhancement of Double Pipe Heat Exchangers by Enforced Turbulence on Single Surface", International Conference Plant Equipment and Reliability, The Equipment Chapter. 27-28, March. Sunway Lagoon, Malaysia 2008.

[9] Veysel Ozceyhan, Sibel Gunes, Orhan Buyukalaca, Necdet Altuntop, "Heat Transfer Enhancement in Tubes Using Circular Cross Sectional Rings Separated from the Wall", Journal of Applied Energy 85 (2008) 988-1001

[10] Kakac, Paykoc, "Basic Relationships for Heat Exchangers", NATO Scientific Affairs Division, Vol 143, pp.29-80, (1988)

[11] Han, J. C., Glicksman, L. R. And Rohsenow, W. M., " An Investigation of Heat Transfer and Friction Factor for Rib-Roughened Surfaces", Int. J. Heat Mass Transfer, Vol. 21, pp.1143-1156,1978.

[12] Webb, R. L., Eckert, E. R. G. And Goldstein, R. J., "Heat Transfer and Friction in Tubes with Repeated-Rib Roughness", Int. J. Heat Mass Transfer, Vol. 14, pp. 601-617, 1971.

[13] H.K.Versteeg, & Malalasekera, W. (1995). An introduction to computational fluid dynamics, the finite volume method. Prentice Hall.

APPENDIX A

PARAMETERS OF ALL INVESTIGATED CASES

Case	Rec	Vel (m/s)	Heat Flux (W/m2)	Pi (Pa)	Tci (C)
S1	20156.45	0.3534186	35774.98446	4951635	35
S2	13285.21	0.2329399	30317.78344	7512668	34.25
S3	10603.88	0.185926	27286.0051	9412345	34
S4	7952.956	0.1394453	23647.87108	12549721	34
S5	5399.311	0.0946703	18797.02573	18485206	34.5
S6	2742.475	0.0480859	12127.11338	36393177	35
R1.1	20201.01	0.3542	51436.56963	4940711	35
R1.2	13285.21	0.2329399	47868.71509	7512668	34
R1.3	10701.12	0.187631	45192.82418	9326816	34
R1.4	8098.967	0.1420055	41624.96964	12323470	34
R1.5	5448.19	0.0955273	36273.18783	18319364	34
R1.6	2760.89	0.0484088	27353.55148	36150436	34.5
R2.1	19156.99	0.3358943	52345.71269	5209972	32
R2.2	12831.56	0.2249857	47587.01154	7778273	32
R2.3	10313.41	0.180833	45207.66096	9677437	32
R2.4	7753.202	0.1359429	41638.63509	12873053	32
R2.5	5253.419	0.0921123	35690.25865	18998556	32
R2.6	2663.117	0.0466945	25280.59988	37477654	32
R3.1	19609.57	0.3438298	54725.06327	5089728	33.25
R3.2	13528.82	0.2372113	49074.10565	7377390	35
R3.3	10798.62	0.1893406	47587.01154	9242605	34.5
R3.4	8245.823	0.1445804	43125.7292	12103992	35
R3.5	5546.319	0.0972479	38664.44687	17995246	35
R3.6	2866.132	0.0502541	29147.04457	34823022	35.75

Table 4   Parameters of all investigated cases

Appendix B

MATLAB MODULE OF THE ANALYTICAL PROCEDURE

```
clc
clear all
option=input('Enter a to use the predefined values or b to use new
values ','s');
poe=input('Enter the p/e ratio ');
if option == 'a'

%@@@@@@@@@@@@@@@@@@@@@@@@@@@@@@@@@@@@@@@@@@@@@@@@@@@@@@@@@@@@@@@@@@@@@@@@@@
                            %PROBLEM PARAMETERS
%@@@@@@@@@@@@@@@@@@@@@@@@@@@@@@@@@@@@@@@@@@@@@@@@@@@@@@@@@@@@@@@@@@@@@@@@@@

e=[0.0025  0.003213 0.0045];
Rec=[20156.45 13285.21 10603.88 7952.956 5399.311 2742.475];
Reh=[42658.23333];


%--------------------------------------------------------------------------


%@@@@@@@@@@@@@@@@@@@@@@@@@@@@@@@@@@@@@@@@@@@@@@@@@@@@@@@@@@@@@@@@@@@@@@@@@@
                            %DATA INPUT
%@@@@@@@@@@@@@@@@@@@@@@@@@@@@@@@@@@@@@@@@@@@@@@@@@@@@@@@@@@@@@@@@@@@@@@@@@@

    %*********************** Predefined Values *****************
       Length = 2;

            %-------------Cold Flow information--------------------
       Tc=308;
       Pwc=5;
       densc=994;
       visc=(0.727*10^-3);
       CPc=4178;
       Prc=4.83;
       Kc=0.623;
            %-------------Hot Flow information------------------
       Th=350;
       Pwh=0.75;
       densh=973.25;
       vish=0.365*10^-3;
       CPh=4195;
       Prh=2.29;
       Kh=0.668000;

else

%*********************User Values ********************

length=input('Enter the length of the pipe---> ');
Do=input('Enter the outer diameter of the pipe---> ');
Din=input('Enter the inner diametere of the piep---> ');

          %------------Cold Flow information-----------------------

Tc=input('Enter the Cold flow temperature---> ');
```

```
Pwc=input('Enter the Cold pump power---> ');
densc=input('Enter the cold flow density ---?');
velc=input('Enter cold flow velocity --->');
visc=input('Enter the cold flow viscosity--- >');
CPc=input('Enter the cold flow Cp--->');
Prc=input('Enter the cold flow Pr---> ');
Kc=input('Enter the cold flow thermal condcutivity ---->');

        %--------------Hot Flow information-----------------------

Th=input('Enter the Hot flow temperature---> ');
Pwh=input('Enter the hot pump power---> ');
densh=input('Enter the hot flow density ---?');
vish=input('Enter the hot flow viscosity--- >');
CPh=input('Enter the hot flow Cp--->');
Prh=input('Enter the hot flow Pr---> ');
Kh=input('Enter the hot flow thermal condcutivity ---->');
end


%----------------------------------------------------------------------

%@@@@@@@@@@@@@@@@@@@@@@@@@@@@@@@@@@@@@@@@@@@@@@@@@@@@@@@@@@@@@@@@@@@@@@@@@@
                        %SMOOTH CASE
%@@@@@@@@@@@@@@@@@@@@@@@@@@@@@@@@@@@@@@@@@@@@@@@@@@@@@@@@@@@@@@@@@@@@@@@@@@

Dh=0.042;
Dhh=0.0254;
Rh=20000;
Rc=20000;
for j=1:length(Reh)


        %--------------Friction Factor--------------------------
for i=1:length(Rec)
    frbc(i)= (0.0791)*((Rec(i))^(-0.25));
    frmcc(i)=0.0014+0.125*Rec(i)^(-0.32);
    frbh(j)= (0.0791)*(Reh(j))^(-0.25);
    frmch(j)=0.0014+0.125*Reh(j)^(-0.32);
    fra=(frbc+frmcc)/2;


        %--------------Nussult Number------------------------------
Nuc(i)= 0.023*((Rec(i))^0.8)*(Prc)^0.4;    % cold side
Nuh(j)= 0.023*((Reh(j))^0.8)*(Prh)^0.3;    % Hot Side


        %--------------Heat Transfer Coefficient----------------
hc(i)=(Nuc(i)*Kc)/Dh;                       % cold side
hh(j)=(Nuh(j)*Kh)/Dhh;                      % Hot Side


        %------------Stanton Number------------------------------

Stc(i)= Nuc(i)/(Rec(i)*Prc);                % cold side
Sth(j)= Nuh(j)/(Reh(j)*Prh);                % Hot Side
    end
end


%----------------------------------------------------------------------

%@@@@@@@@@@@@@@@@@@@@@@@@@@@@@@@@@@@@@@@@@@@@@@@@@@@@@@@@@@@@@@@@@@@@@@@@@@
                        %RRIBBED CASE
%@@@@@@@@@@@@@@@@@@@@@@@@@@@@@@@@@@@@@@@@@@@@@@@@@@@@@@@@@@@@@@@@@@@@@@@@@@

frrc=zeros(size(e));
```

```
for j=1:length(e)
    for i=1:length(Rec)
        ep=1;
        limit=1;
        while limit > 0.001
            if ep<35
                m=-0.4;
            else
                m=0;
            end

            if poe<10
                n=-0.13;
            else
                n=0.35;
            end

            frrc(i,j) = 2/(((3.300722/(10/poe)^n) * (ep/35)^(m)- 2.5
* log(2*e(j)/Dh) - 3.75)^2);

            epc= (e(j)/Dh)* Rec(i)* (frrc(i,j)/2)^0.5;

            limit=abs((epc - ep)/ep);
            ep=epc;

        end
        eplus(i)=ep;

        if eplus(i)<35
            m=-0.4;
        else
            m=0;
        end

        if eplus(i)<35
            d= 1;
        else
            d= 0.28;
        end

        if poe<10
            n=-0.13;
        else
            n=0.35;
        end
        Replus(i)= (3.300722/((poe/10)^n))*(eplus(i)/35)^m;
% (Roughness Function)
        Hew(i,j)=4.5*((eplus(i))^0.28)*(Prc^(0.57));       % (Web
Correlation)
        Heh(i,j)=(8*(eplus(i)/35)^(d))/(2)^(-0.45);        % (Han
Correlation)

        stw(i,j)= frrc(i,j)/(((Hew(i,j)-
Replus(i))*((2*frrc(i,j))^(0.5)))+2);    %Stanton Number with Web
correlation
        sth(i,j)= frrc(i,j)/(((Heh(i,j)-
Replus(i))*((2*frrc(i,j))^(0.5)))+2);    %Stanton Number with Han
correlation
        sta=(stw+sth)/2;

    end
end
```

```
for j=1:length(e)
    for i=1:length(Rec)
        enhst(:,j)=stw(:,j)./Stc';
        enhfr(:,j)=frrc(:,j)./fra';
    end
end
```

Appendix C

MATLAB MODULE OF THE NUMERICAL PROCEDURE

```
%**************** GEOMETRY INFORMATION****************
Dh=0.042;
Dhh=0.0254;
Do=0.0342;
Ah=pi*2*Do;
Ks=30.7;


    %--------------Cold Flow information-------------------
    Pwc=5;
    densc=994;
    visc=(0.732*10^-3);
    CPc=4178;
    Prc=4.91;
    Kc=0.624;
            %--------------Hot Flow information-----------------
    Pwh=0.75;
    densh=973.25;
    vish=0.365*10^-3;
    CPh=4195;
    Prh=2.29;
    Kh=0.668000;


%**************** h FOR HOT FLOW****************************
velhot=vish*Reh/(densh*Dhh);
mh=densh*velhot*pi*(Dhh^2)/4;
hh=0.023*Reh^(0.8)*Prh^(0.3)*Kh/Dhh;


for i=1:length(Tci)
      delth(i)=Thi(i)-Tho(i);
      deltc(i)=Tco(i)-Tci(i);
      velcold(i)=visc*Rec(i)/(densc*Dh);
      mc(i)=densc*velcold(i)*pi*(Dh^2)/4;
      delta(i)= Tho(i)-Tci(i);
      deltb(i)= Thi(i)-Tco(i);
      LMTD(i) = (deltb(i)-delta(i))/log(deltb(i)/delta(i));    %----
-------- LMTD------------------

Q(i)=mh*CPh*delth(i);

uo(i)= Q(i)/(Ah*LMTD(i));

a=(Do/(Dhh*hh))+0.5*Do*(log(Do/Dhh))/Ks;
ho(i)=(uo(i)^(-1)-a)^(-1);

Nuc(i)= ho(i)*Dh/Kc;
Stc(i)= Nuc(i)/(Rec(i)*Prc);
%
delp(i)= abs(pe(i)-po(i));
f(i)=delp(i)/((8*500*(vel(i))^2)/0.042);
end
```

APPENDIX D

SIMULATION RESULTS

Case	To (exp)	To (num)	Pi	Po	Vm	Delta P	St (exp)	St (num)	St (Webb)	fr (exp)	fr (num)	fr (Webb)
R 1.1	36.75	37.11	25.220	-630.911	0.3057	656.131	0.0036	0.0037	0.0039	0.0842	0.0737	0.0843
R 1.2	36.25	37.00	10.869	-296.785	0.2010	307.654	0.0041	0.0042	0.0043	0.0855	0.0800	0.0843
R 1.3	37	37.53	7.214	-223.222	0.1630	230.436	0.0044	0.0044	0.0046	0.0857	0.0911	0.0843
R 1.4	38	38.40	4.117	-129.092	0.1234	133.209	0.0048	0.0047	0.0050	0.0852	0.0919	0.0843
R 1.5	39	39.67	1.841	-64.525	0.0830	66.366	0.0055	0.0052	0.0055	0.0854	0.1012	0.0843
R 1.6	40	42.97	0.470	-18.816	0.0421	19.286	0.0067	0.0065	0.0065	0.0836	0.1143	0.0816
R 2.1	34	34.3016	21.4774	-667.977	689.455	0.335894	0.00315	0.0033	0.0035	0.0655	0.0642	0.0692
R 2.2	34.5	35.0807	9.216306	-320.674	329.890	0.224986	0.00353	0.0037	0.0039	0.0668	0.0684	0.0692
R 2.3	35	35.6688	5.840482	-220.722	226.562	0.181	0.00388	0.004	0.0042	0.0666	0.0726	0.0692
R 2.4	35.25	36.4126	3.501422	-131.955	135.457	0.135943	0.00428	0.0044	0.0045	0.0667	0.0578	0.0692
R 2.5	37	37.7147	1.729912	-48.0847	49.815	0.092112	0.00478	0.0047	0.005	0.0657	0.0616	0.0692
R 2.6	38.5	39.7213	0.4288	-12.7309	13.160	0.046694	0.00544	0.0052	0.0057	0.0646	0.0634	0.0618

S1.1	36.5	36.4365	-0.30152	-93.997	93.69551	0.353419	0.0013	0.0012	0.0012	0.0068	0.0079	0.0066
S1.2	36	36.4225	-0.15257	-46.3716	46.21906	0.23294	0.0014	0.0013	0.0013	0.0075	0.0089	0.0074
S1.3	36	37.4685	-0.10749	-31.5665	31.45902	0.185926	0.0015	0.0014	0.0014	0.0078	0.0096	0.0078
S1.4	36	36.7603	-0.06949	-19.5253	19.45579	0.139445	0.0016	0.0015	0.0015	0.0085	0.0105	0.0084
S1.5	37.5	37.3465	-0.04044	-10.5101	10.46962	0.09467	0.0018	0.0016	0.0016	0.0095	0.0123	0.0093
S1.6	38.57	38.6278	-0.0172	-3.93898	3.921782	0.048086	0.0020	0.0019	0.0018	0.0115	0.0178	0.0111
R3.1	35.75	35.5554	-2.16123	-1016.43	1014.265	0.34383	0.00412	0.0044	0.0044	0.179	0.0901	0.1728
R3.2	37.25	37.9896	-1.05499	-533.037	531.9822	0.237211	0.00484	0.0049	0.0049	0.180	0.0993	0.1728
R3.3	37.5	38.1259	-0.68651	-346.324	345.6374	0.189341	0.00537	0.0054	0.0052	0.184	0.1012	0.1728
R3.4	39	39.3011	-0.43074	-207.399	206.9678	0.14458	0.00581	0.0055	0.0057	0.180	0.104	0.1728
R3.5	40	40.7065	-0.20621	-103.765	103.5589	0.097248	0.00674	0.0064	0.0063	0.179	0.115	0.1728
R3.6	43	44.0559	-0.06357	-32.5634	32.4998	0.050254	0.00825	0.0075	0.0076	0.181	0.1351	0.1728

Table 5   Simulation results

Case	η/τ (num)	η/τ (exp)	η/τ (anal)	Str/St (num)	Str/St (exp)	Str/St (anal)
R 1.1	9.329	12.437	12.693	3.083	2.679	3.135
R 1.2	8.989	11.446	11.422	3.231	2.901	3.229
R 1.3	9.490	10.945	10.783	3.143	3.007	3.281
R 1.4	8.752	10.071	10.013	3.133	3.038	3.347
R 1.5	8.228	9.027	9.054	3.250	3.114	3.438
R 1.6	6.421	7.270	7.330	3.421	3.323	3.554
R 2.1	8.127	9.675	10.427	2.750	2.351	2.866
R 2.2	7.685	8.942	9.383	2.846	2.504	2.946
R 2.3	7.563	8.506	8.858	2.857	2.639	2.989
R 2.4	5.505	7.884	8.225	2.933	2.709	3.044
R 2.5	5.008	6.945	7.438	2.938	2.716	3.118
R 2.6	3.562	5.617	5.551	2.737	2.706	3.103
R 3.1	11.405	26.440	26.182	3.667	3.075	3.667
R 3.2	11.157	24.096	23.351	3.769	3.433	3.769
R 3.3	10.542	23.499	22.154	3.857	3.653	3.714
R 3.4	9.905	21.277	20.571	3.667	3.677	3.800
R 3.5	9.350	18.922	18.581	4.000	3.830	3.938
R 3.6	7.590	15.739	15.568	3.947	4.104	4.222

Table 6   Simulation results